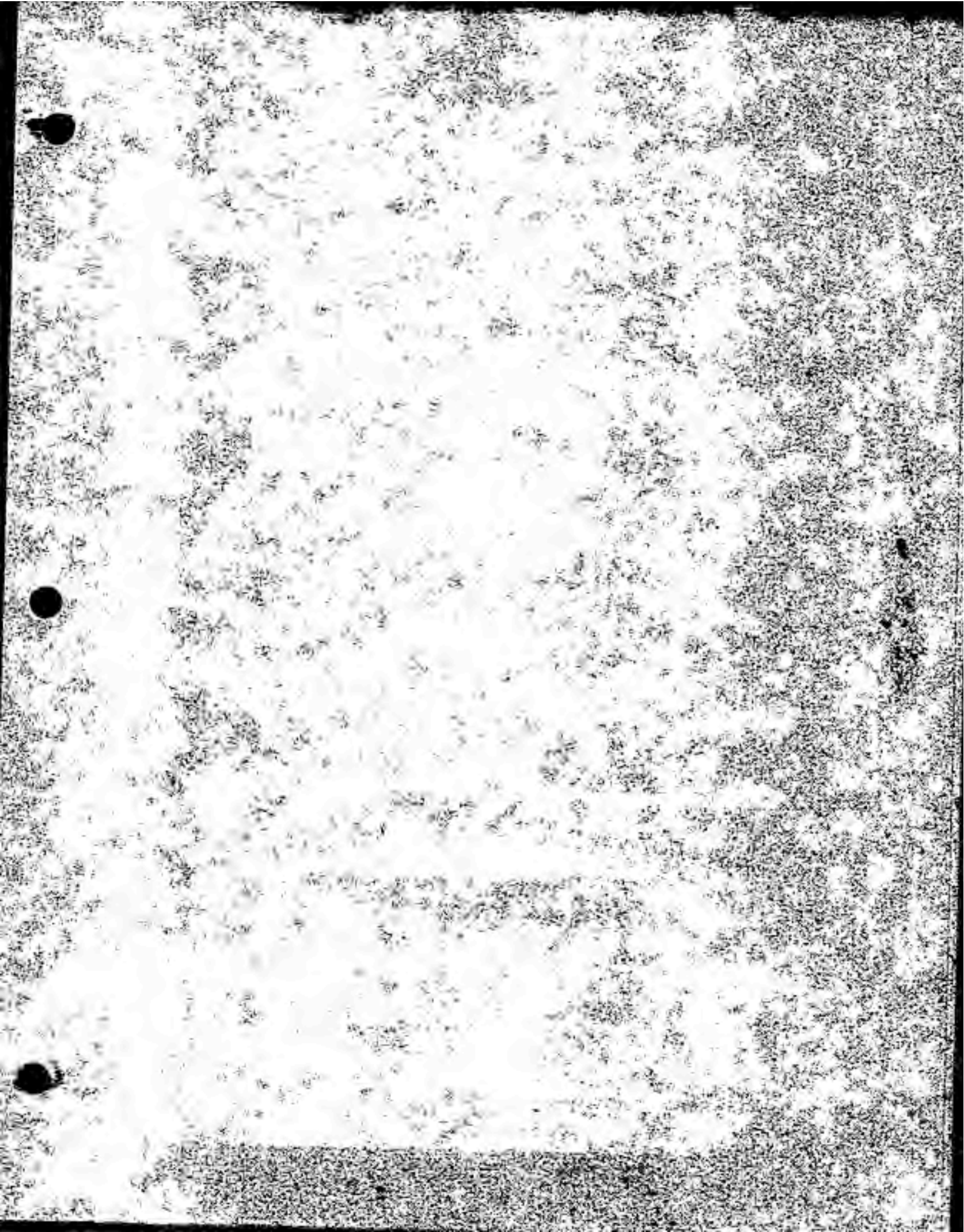

ABSTRACT

JAMES B. GARBER. Testing of a Multicomponent Model of Adsorption and Biodegradation of Natural Organic Matter on Activated Carbon. (Under the Direction of Dr. Francis A. DiGiano)

Adsorption and biodegradation studies were performed to characterize the components present in natural organic material (NOM) obtained from Lake Drummond, in southeastern Virginia.

NOM adsorbability was characterized by dividing it into fictive components, using the Ideal Adsorbed Solution Theory (IAST) to find the Freundlich parameters and initial concentration of each. This was done for ozonated and ozonated-biostabilized NOM. The isotherm results, along with the results of the biokinetic experiment, were used to determine the components of the model NOM solution.

A batch biokinetic study was performed to determine the biokinetic parameters for the ozonated NOM solution. A first-order model was fit to the experimental data, giving a first-order rate constant, yield coefficient, and coefficient of microbial decay for the biodegradable fraction of the NOM.

A multicomponent model developed by Pedit (1988) was tested using the experimentally determined adsorption and biodegradation parameters. The model failed to predict the breakthrough of total organic carbon (TOC) and the resulting total inorganic carbon (TIC) production when the biodegradable fraction of NOM was assumed to be 55 percent,

as determined using a continuous flow GAC reactor which had apparently reached an exhaustion of adsorption capacity. The model results were improved when the biodegradable fraction was assumed to be 15 percent, as obtained from the batch biokinetic experiment. This suggests that slow adsorption, in addition to biodegradation, may have been responsible for long term TOC removal in the continuous flow GAC reactor.

ACKNOWLEDGEMENTS

I would like to express my appreciation to my advisor, Dr. DiGiano, for his technical guidance during this project, and for his patience during the long distance completion of the report itself. I would also like to thank Dr. Miller and Dr. Aitken for their input during the execution of the experimental work, and for their comments on the draft of the report. In addition, I would like to thank Joe Pedit, who developed the mathematical model used in this work, Jan DeWaters, for loaning me her lab notes while she was overseas, Greg Harrington, for his input during the isotherm studies, and Stephan Grimberg, for assisting with sample collection.

The time I spent in Chapel Hill was made memorable and rewarding by Andy Lawler, Dan Elliott, Kathy Dolce, Fred Corn, Daniel Lopez-Rendon, Pierre Tristam, and others, who provided the necessary distractions from studies and the lab. The nights in the basement labs of Rosenau were made bearable, even entertaining, by the other members of "the night shift," to whom I may owe my sanity.

My sincerest appreciation goes to Rebecca, my wife, who has endured both our 700 mile engagement, and my sometimes single-minded determination to complete this report while working full time.

Finally, thanks to my family for their support in this and other pursuits.

TABLE OF CONTENTS

LIST OF TABLES

LIST OF FIGURES

CHAPTER 1. INTRODUCTION AND OBJECTIVE

1.1 Introduction

In May of 1989 the United States Environmental Protection Agency (USEPA) proposed national primary drinking water standards for 30 synthetic organic chemicals (SOCs) in compliance with the 1986 Amendments to the Safe Drinking Water Act. Granular activated carbon (GAC) treatment is considered a best available technology (BAT) for the removal of 28 of these chemicals by USEPA. In addition, the maximum contaminant level for total trihalomethanes (THMs), currently 100 ug/L, may be lowered in 1990.

The removal of natural organic matter (NOM) by GAC plays an important role in controlling SOCs and THMs. First, NOM is the precursor material for THMs, and thus its removal is desirable. In addition, NOM often confounds the predictability of GAC performance with respect to SOC removal by coating the GAC surface, thereby preventing effective adsorption of SOCs (Zimmer, Brauch, and Sontheimer, 1989) and decreasing bed life. Furthermore, since NOM does not adsorb well, GAC is not effective for its removal.

Ozonation of NOM has been shown to increase its biodegradability. This not only improves NOM removal, but may also improve removal of SOCs. SOCs, if present at concentrations below the level required to support growth (S_{min}), may be degraded in the presence of other compounds, such as NOM, present at concentrations greater than S_{min} (Namkung and Rittmann, 1987b). Adsorption of SOCs is also enhanced when biodegradation of NOM diminishes the extent of surface fouling.

The major difficulty in modeling NOM behavior has been its heterogeneous nature, the result of a wide range of molecular weights and chemical characteristics, and corresponding spectra of adsorbability and biodegradability. In order to predict the influence of NOM on GAC adsorber performance, therefore, it is necessary to determine adsorption and biokinetic parameters which adequately characterize the NOM present in solution.

1.2 Objective

This research is intended to provide a better understanding of the adsorption and biodegradation of ozonated NOM in a continuous flow GAC reactor. The approach taken is to consider NOM as a mixture of pseudo-components, as has been done by others (Hubele, 1985; Harrington and DiGiano, 1989) in analyzing adsorption characteristics. This concept is extended here to analyze biodegradation

characteristics as well. Experimentally determined adsorption and biokinetic parameters for the pseudo-components are used to test the Multicomponent Adsorption and Biodegradation (MCAB) Model developed for this research by Joseph Pedit, a PhD student in the Department of Environmental Science and Engineering at the University of North Carolina at Chapel Hill.

CHAPTER 2. BACKGROUND

2.1 Natural Organic Matter

Natural organic matter (NOM) is organic material which occurs naturally in both surface water and groundwater. Soil humus, primarily produced by the degradation of plant matter, is a significant source of NOM in water through both surface runoff and percolation. Thus, the characteristics of NOM are a function of the vegetation, microbial population, and the physical/chemical nature of the soils in a watershed. Once in water the character of the organic matter can be altered by ultraviolet irradiation, biodegradation, and adsorption to minerals.

Several terms have been used in the literature to refer to this material, including humic substances, background organic matter, and dissolved organic matter. This heterodisperse group of compounds is, in lieu of a specific molecular description, operationally defined by total organic carbon (TOC), and to a lesser degree by color.

2.2 Importance of NOM in Drinking Water Treatment

NOM has long been of concern in water treatment. The first regulation of NOM in the United States was under the heading of color, as a secondary standard of the Public Health Service Standards of 1925. From 1925 until the mid 1970's NOM was considered only an aesthetic problem.

The concern over NOM shifted from an aesthetic to a public health issue when Rook (1974) associated it with the formation of chloroform and other trihalomethanes (THMs) upon chlorination. THMs were soon measured in finished water throughout the United States (Symons, et al., 1975). The THMs, a group of known carcinogens, is the most common of the 12 known classes of disinfection by-products. The total THMs are regulated as a primary contaminant under the Safe Drinking Water Act (SDWA) of 1974, and are subject to a maximum contaminant level (MCL) of 0.10 mg/L. To comply with the 1986 amendments to the SDWA, the United States Environmental Protection Agency (USEPA) has proposed new MCLs for many synthetic organic chemicals (SOCs), and is expected to lower the MCL for THMs in 1990 or 1991, possibly to 0.05 mg/L or less.

In addition to the formation of undesirable by-products as a result of chlorination, NOM can interfere with the removal of target organic compounds in granular activated carbon (GAC) adsorbers. A study of full scale GAC columns showed that the adsorption capacity for trichloroethene,

tetrachloroethene, and 1,1,1-trichloroethane was significantly reduced in the presence of NOM (Zimmer, Brauch, and Sontheimer, 1989). This was attributed to the coating of the GAC by NOM, which prevents effective adsorption of target organics. In another study (Summers, et al., 1989), the amount of trichloroethene adsorbed in a GAC column was substantially less than predicted in an equilibrium batch isotherm study, reportedly due to a component of NOM that penetrates more deeply into the GAC bed and fouls adsorptive capacity. This fouling, which decreases adsorption capacity and bed life, in addition to other aspects of the complex relationship between NOM and SOCs, makes it necessary to understand the characteristics and behavior of NOM in GAC adsorbers.

2.3 Characterization of NOM

NOM is a heterodisperse mixture which displays a wide range of molecular weights, and consists of components with varying degrees of biodegradability and adsorbability. It is difficult to isolate and characterize the components of NOM. One approach which has proven useful for separating the fractions of NOM is gel permeation chromatography, a method which fractionates the NOM on the basis of apparent molecular weight (AMW). This method has been used to show that NOM exhibits a range of AMWs from less than 1000 to greater than 40,000 (Veenstra, Barber, and Kahn, 1983). All

of the chromatograms showed a peak in the approximate range of 1,000 to 5,000, with the highest TOC concentration occurring in the 1,000 to 3,000 range. Similar patterns and molecular weight distributions have been reported by other researchers (Brogden, 1971; Davis and Gloor, 1981).

Chromatograms for ozonated and non-ozonated water samples were used to construct cumulative probability plots of AMW versus the percent of the TOC of AMW less than the specified AMW. Veenstra's results suggested that ozone causes a shift in the molecular weight distribution toward lower molecular weights. An overall TOC reduction of 9.4 percent, along with a decrease in the fraction of TOC in the less than 1,000 AMW range, indicate that a fraction of the organic matter in this range is completely oxidized to CO_2 and water. Neukrug et al. (1984) measured an 11 percent TOC reduction across a pilot scale ozone contactor (following clarification and rapid sand filtration). Mallevialle (1982) observed a 5.6 percent TOC reduction in a similar system.

Another approach to characterizing NOM mixtures is to use multicomponent equilibrium models, such as the ideal adsorbed solution theory (IAST) model (Radke and Prausnitz, 1972). In this approach, NOM is considered as a mixture of fictive, or pseudo-components (PCs). IAST is used to find the Freundlich adsorption parameters and initial concentration of each PC in the NOM mixture. Harrington and DiGiano (1989) used this approach to examine the effect of

coagulation, and various levels of ozonation and biodegradation, on the equilibrium adsorption behavior of NOM. This approach was not entirely successful for obtaining a systematic relationship between adsorbability and ozone dosage. Hubele (1985) used a similar approach to study the adsorbability of ozonated humic substances. A set of five PCs was used for isotherm evaluation. Identical Freundlich 1/n parameter values were assumed for all PCs, while each PC was assigned a different K value. With these preset adsorption parameters, concentrations of the PCs were determined using non-linear regression. Using this approach, a linear relationship between ozone dose and the concentration of each PC was established.

2.4 Effect of Ozone on Biodegradation and Adsorption of NOM

Since NOM has been shown to interfere with the adsorption of target compounds on GAC, and because NOM itself is poorly adsorbed, GAC does not provide an effective means for its removal. Ozone has been shown to increase the biodegradability of NOM. Hubele (1985) reported that ozone increased the biodegradability and decreased adsorbability of NOM. Increasing ozone dose has also been shown to increase the non-adsorbable fraction of NOM, and decrease the concentration of better adsorbing substances (Zimmer, Brauch, and Sontheimer, 1989). The oxidation reaction leads to more polar molecules, which helps to explain the

increased biodegradability and decreased adsorbability of ozonated NOM. Several other authors have reported an increase in biodegradability upon ozonation, including Benedek (1979) and Somiya et al. (1983).

In GAC processes treating ozonated NOM there is often significant, long term steady-state TOC removal. DeWaters (1987) showed that ozonated NOM can serve as the primary substrate for a biofilm grown on GAC. For an apparent ozone dose of 1.1 mg/mg TOC, and an empty bed contact time of 3.9 minutes, over 30 percent of the influent TOC was removed at steady state. Glaze and Wallace (1984) reported that columns fed ozonated water performed better than columns fed unozonated water when biological processes predominated. Benedek (1977) reported that ozonation had little effect on TOC reduction due to the simultaneous increase in biodegradability and decrease in adsorbability, but explained that an insufficient ozone dosage or prechlorination of the water may have been responsible.

Another theory for long term steady state removal and the resulting extended bed life is slow adsorption kinetics. Slow adsorption is the diffusion of an adsorbate, such as NOM, into the micropores of the GAC particle. Neukrug et al. (1984) reported that biodegradation and slow adsorption appear to play key roles when the adsorbent surface is nearly saturated. Maloney et al. (1984) studied biologically active filters with GAC and sand media at warm and cold temperatures to distinguish between biodegradation

and slow adsorption as causes of long term TOC removal. They reported that about 20 percent of the feed TOC was removed by slow adsorption, and that between 8.5 and 16 percent was removed by biodegradation. Peel and Benedek (1980), assuming slow adsorption is the result of a resistance to intraparticle diffusion in the GAC micropores, used isotherm and batch kinetic data to determine two intraparticle diffusion parameters to describe adsorption of phenol and chlorophenol.

2.5 Modeling of Adsorption and Biodegradation on GAC

Several mathematical models featuring biodegradation and adsorption have been developed. Early single component models (Benedek, 1979; Ying et al., 1978) considered an adsorbable, biodegradable solute present at relatively high concentrations. Speitel, Dovantzis, and DiGiano (1987) developed a single component model to investigate the bioregeneration of GAC. Hubele (1985) formulated a model capable of handling more than one component simultaneously. Using this approach, it is possible to describe the behavior of a mixture of solutes, each possessing different adsorption and biodegradation characteristics.

Chang and Rittmann (1987) used a single-component model to study the adsorption and biodegradation of phenol and acetate at low concentrations in a completely mixed fixed film reactor. This reactor configuration, while probably of

little practical use in field installations, is useful for laboratory research because it simplifies the collection and analysis of biokinetic data, i.e. the effect of axial distance on substrate concentration profiles and biodegradation rate is minimized. In a model developed by Pedit (1988), the model of Chang and Rittmann was expanded to include as many as four components, using a finite element solution technique instead of the orthogonal collocation method used by Chang and Rittmann.

CHAPTER 3. SAMPLE COLLECTION, STORAGE, AND PREPARATION

3.1 Sample Collection and Storage

Water high in NOM was obtained on February 2, 1988 from Lake Drummond, located in the Great Dismal Swamp in southeast Virginia. The area had experienced no major storms prior to the sampling trip, so the water collected was assumed to represent average February conditions. The water temperature was approximately 40° F.

The water was returned to Chapel Hill within 8 hrs and placed in cold storage at 4° C. The next day all of the water was filtered through a 1.0 um honeycomb filter to remove suspended material. The resulting pre-filtered water was returned to storage at 4° C for future use. The average TOC of the filtered samples was 38.4 mg/L.

3.2 Sample Preparation

A 40 L sample was ozonated in two, 20 L batches for use in biokinetic and adsorption experiments. An apparent ozone dose(AOD) of 1 mg O_3/mg TOC was obtained by sparging ozone produced by a Grace LG-2-LI laboratory ozone generator (Union Carbide, South Plainfield, NJ) into each 20 L batch.

A schematic of the apparatus used is shown in Figure 3.1.

The ozonation procedure is described below.

1. 20 L of lake water was placed in the reaction vessel, and each of the four gas washing bottles in the primary and secondary circuits was filled with 500 mL of 40 g/L KI solution.

2. The ozone generator was started and allowed to equilibrate for 5 - 15 minutes by routing the gas flow to vent.

3. The O_3 generation rate was measured by routing the gas through the secondary circuit for 5 minutes. The concentration of ozone in each trap (from which the mass was calculated) was determined using the Iodimetric Method for ozone residual (Standard Methods, 17th ed., 1989). The initial generation rate was then calculated as mass O_3 trapped/5 minutes.

4. The reaction time required to achieve the desired O_3 dosage was calculated based on a dosage of 1 mg O_3/mg TOC, the initial generation rate, an initial TOC concentration, and an assumed gas transfer efficiency. The distribution valve was turned to the primary circuit, allowing ozone to pass through the reaction vessel and associated KI traps.

5. At the end of the predetermined reaction period, the valve was switched to the secondary circuit, and the generation rate was again measured as in step 3. Following this the ozone generator was shut off.

6. The reaction vessel was then purged with nitrogen gas to strip any ozone remaining in solution. Titration of the KI traps in the primary circuit yields the mass of ozone trapped during the course of ozonation of the 20 L sample. This mass was the sum of the ozone which passed through the sample without going into solution and that in solution but purged at the end.

The apparent ozone dose was calculated as the difference between the mass of ozone supplied and that trapped by the KI solution, divided by the mass of TOC in the untreated water.

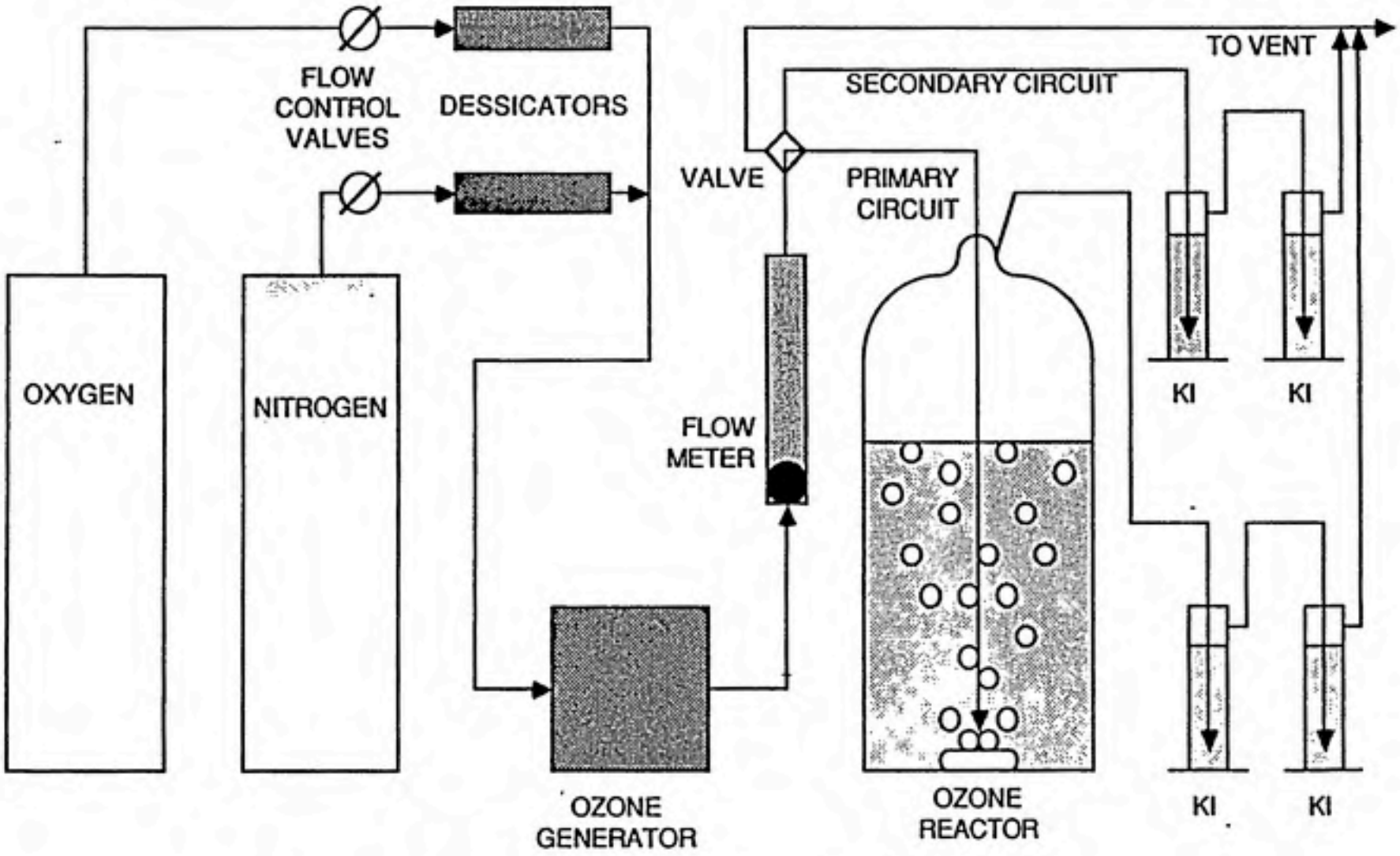

Figure 3.1 Schematic of Ozonation Apparatus (from Harrington and DiGiano, 1989).

$$AOD = ((r_g * t_r) - M_{out})/(TOC_0 * V_r) \quad (3.1)$$

where: r_g = O_3 generation rate (g/hr)

t_r = reaction time (hr)

M_{out} = Mass O_3 trapped by KI solution (g)

TOC_0 = Initial TOC (mg/L)

V_r = Volume of reaction vessel (L)

Ozonation tended to reduce the TOC of the samples. The average TOC in the four jugs used in this research prior to ozonation was 38.4 mg/L. Ozone applied at approximately 1 mg/mg TOC destroyed an average of 5.7% of the initial TOC, leaving the average TOC of the ozonated samples at 36.2 mg/L.

CHAPTER 4. RATIONALE FOR EXPERIMENTAL DESIGN

4.1 Description of Pseudo-Components

The two characteristics of the NOM most important with respect to their behavior in a biologically active GAC bed are biodegradability and adsorbability. There is no single set of biokinetic or adsorption parameters which can completely describe a particular NOM solution. Natural organic matter embodies a wide range of molecular weights, from less than 1000 to greater than 40,000. It is reasonable, therefore, to expect that the biodegradability and adsorbability of these fractions will vary. Because the exact molecular configuration of each NOM fraction is unknown, the concept of pseudo-components has been used by others (Hubele, 1985; Harrington and DiGiano, 1989). This concept, however, has for the most part been restricted to the analysis of adsorbability; the goal here is to extend this concept to the analysis of biodegradability. The simplest set of pseudo-components

would divide NOM into the following:

1. Adsorbable, non-Biodegradable (A/NB)
2. Biodegradable, non-Adsorbable (B/NA)
3. Adsorbable, Biodegradable (A/B)
4. Non-Biodegradable, non-Adsorbable (NB/NA)

The breakthrough pattern of each component from a continuous flow reactor containing GAC media can be hypothesized as in Figure 4.1. The sum of the feed concentrations to the GAC bed is given by:

$$C_T = C_{A/B} + C_{A/NB} + C_{NA/B} + C_{NA/NB} \qquad (4.1)$$

where the subscripts refer to the four components defined above. The adsorbable, non-biodegradable component (Component A/NB) will exhibit a pattern of breakthrough like any non-biodegradable adsorbate: effluent concentration will increase as the adsorption capacity of the GAC is depleted, until finally no further adsorption can occur, and the effluent concentration is equal to the influent concentration.

Breakthrough of the biodegradable, non-adsorbable component (Component A/NB) is complete initially because no biofilm exists on the GAC. As the biofilm becomes established there will be a decrease in the effluent concentration due to biodegradation. A steady-state will

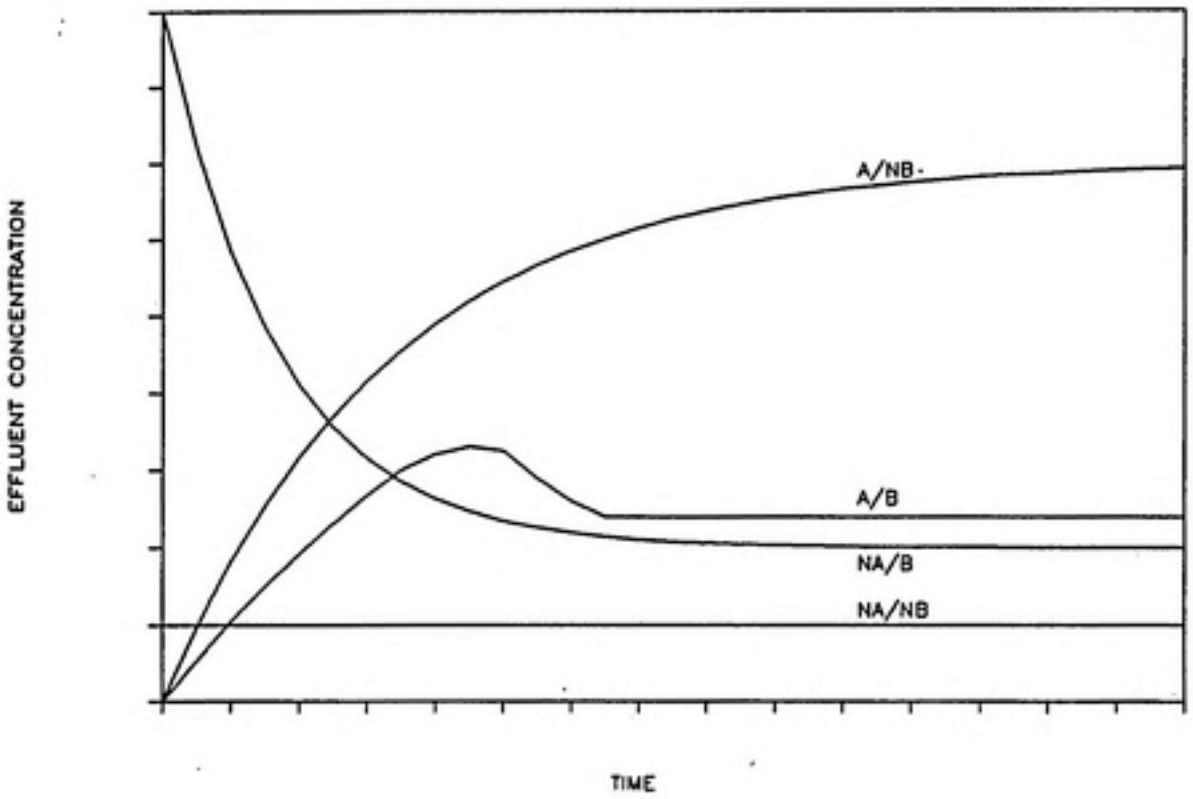

Figure 4.1 Hypothetical Breakthrough Pattern of NOM Pseudo-Components.

eventually be reached with regard to biofilm growth and shearing so as to achieve a constant effluent concentration. The extent of removal of this component will be determined by biokinetics and residence time in the GAC bed.

Initially, breakthrough of the component that is both adsorbable and biodegradable (Component A/B) follows the pattern of the adsorbable, non-biodegradable component (Component A/NB). However, as the biofilm begins to grow, removal is accomplished by both adsorption and biodegradation. Eventually, adsorption is not important, either because adsorption sites have been exhausted or because the biofilm activity is sufficient to eliminate the component before it enters the adsorption space. Biofilm growth, therefore, will account for steady-state removal and prevent complete breakthrough as would be the case for an adsorbable, non-biodegradable component. The extent of removal at steady-state depends on biokinetics and residence time in the GAC bed.

The non-adsorbable, non-biodegradable component (Component NA/NB) is unaffected by either biodegradation or adsorption. Therefore, the effluent and influent concentrations are the same throughout the operating time of the GAC bed.

4.2 Experimental Design

Viewing NOM as a mixture of four pseudo-components, an experimental design was sought to characterize each. The parameters to be determined were: concentration, biodegradability, and adsorbability. These were obtained by batch biokinetic and batch equilibrium adsorption experiments. The expected results of a batch biokinetic experiment are given in Figure 4.2. The initial NOM concentration, $C_T(0)$, is reduced over time by the microbial population to a final concentration of C_{NB}. Therefore, C_{NB} is the concentration of non-biodegradable NOM. The rate at which C_{NB} is approached provides information to determine biokinetics.

Equilibrium adsorption is commonly obtained by the bottle-point procedure, by which various dosages of activated carbon are added to a solution having a fixed initial concentration of the sorbate (in this instance NOM). The result is an adsorption isotherm showing amount adsorbed as a function of equilibrium solution concentration. The experimental design includes construction of adsorption isotherms using both ozonated and ozonated-biostabilized NOM solutions. The initial NOM concentrations before (C_1) and after (C_2) biostabilization can be represented by the

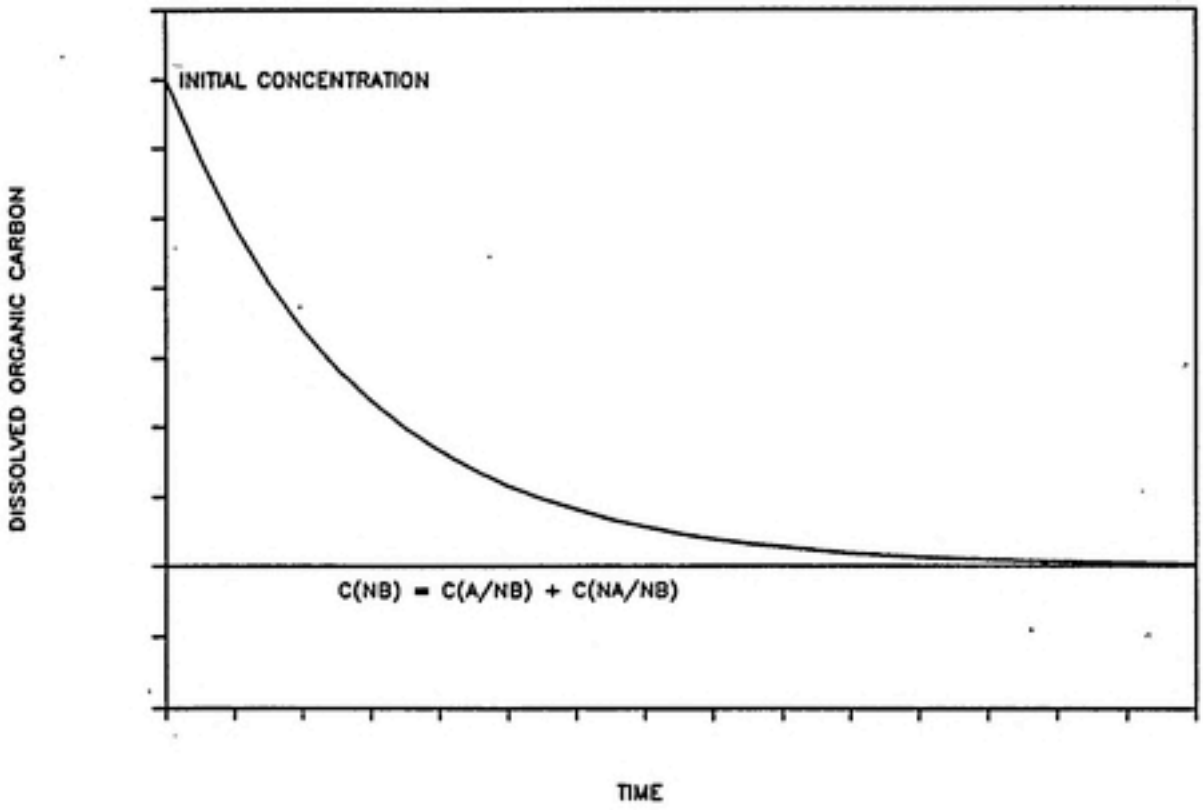

Figure 4.2 Expected Results of Batch Biokinetic Experiment.

following fractions defined earlier:

$$C_1 = C_{A/B} + C_{A/NB} + C_{NA/B} + C_{NA/NB} \quad (4.2)$$

$$C_2 = C_{A/NB} + C_{NA/NB} \quad (4.3)$$

The difference between C_1 and C_2 is due to removal of the two biodegradable fractions:

$$C_1 - C_2 = C_{A/B} + C_{NA/B} \quad (4.4)$$

The general shape and positions of these adsorption isotherms is shown in Figure 4.3. The initial concentration of the ozonated NOM solution is higher than that of the ozonated-biostabilized solution and thus, the adsorption isotherm for ozonated NOM is expected to lie to the right of the isotherm for ozonated-biostabilized NOM.

Experience with NOM isotherms suggests the curvilinear pattern depicted in Figure 4.3 (Harrington and DiGiano, 1989). At high dosages of activated carbon, the residual concentration can be interpreted as the non-adsorbable fraction. The isotherm becomes vertical because no further decrease in bulk phase equilibrium NOM concentration (C_e) occurs with increasing carbon dosage (W). Thus, the equilibrium mass loading, q_e, must correspondingly decrease. The non-adsorbable fraction of NOM is therefore obtained experimentally by projecting the isotherm to the abscissa. For the isotherm obtained using ozonated NOM, the non-

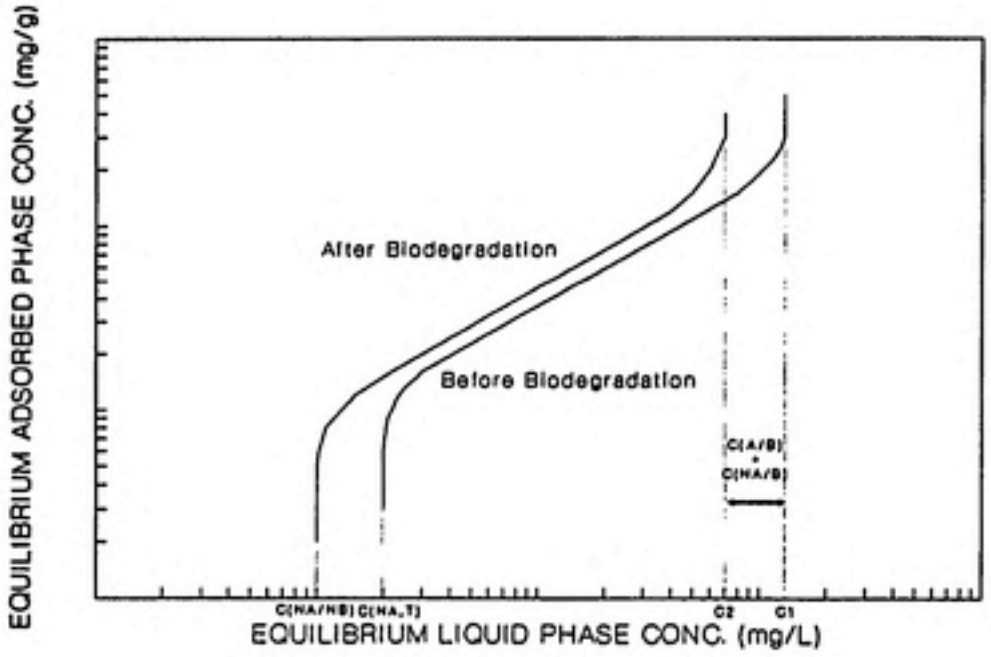

Figure 4.3 Expected Adsorption Isotherms for Ozonated and Ozonated-Biostabilized NOM.

adsorbable fraction is $C_{NA,T}$, as shown in Figure 4.3. That is , $C_{NA,T}$ represents the total non-adsorbable fraction comprised of two components:

$$C_{NA,T} = C_{NA/B} + C_{NA/NB} \qquad (4.5)$$

The non-adsorbable, non-biodegradable fraction, $C_{NA/NB}$, is also obtainable directly from the isotherm experiment by once again projecting the isotherm for the ozonated-biostabilized NOM to the abscissa of Figure 4.3. Thus, the non-adsorbable, biodegradable fraction can be obtained by calculation:

$$C_{NA/B} = C_{NA,T} - C_{NA/NB} \qquad (4.6)$$

Finally, the experimental data allow an inference as to the characteristics of the fraction removed by biostabilization, i.e. (C_1-C_2), as given by Equation 4.4. If the sum of $C_{A/B}$ and $C_{NA/B}$, which is experimentally obtained and shown as Equation 4.4, is equal to $C_{NA/B}$, which is calculated from Equation 4.6, then all of the NOM removed through biostabilization is non-adsorbable. But if $(C_{A/B} + C_{NA/B})$ is greater than $C_{NA/B}$, then the NOM removed through biostabilization consists of both adsorbable and non-adsorbable components.

CHAPTER 5. DETERMINATION OF BIOKINETIC PARAMETERS

5.1 Experimental Method

A batch experiment was performed to determine the biokinetic parameters for the bacteria capable of degrading ozonated NOM. An experimental and a control reactor were used, each being a 4 L erlenmeyer flask. Mixing was provided by magnetic stirrers. Rubber stoppers, with large holes stuffed with glass wool, were used to cap the reactors. This allowed ventilation, while preventing atmospheric contamination of the NOM solution. The initial dissolved organic carbon (DOC) concentration of the NOM solution was 31 mg/L. Both reactors were buffered to a pH of 6.5 using KH_2PO_4 AND Na_2HPO_4; $CaCl_2$, $MgSO_4$, and NH_4Cl were added to provide nutrients. Sodium azide (10 mg/L) was added to the control reactor to inhibit biological activity. A bacterial seed was obtained from a continuous flow GAC reactor, which had been fed the same NOM solution for a period long enough to establish biodegradation, as suggested by CO_2 through the reactor. At the beginning of the experiment, 0.04 g (wet weight) of GAC was transferred from the inlet end of the continuous flow reactor to the experimental and control reactors. After the reactors had

been seeded, DOC and bacterial number were monitored over time. Bacterial number was determined using the Direct Total Count procedure, a method widely used in the counting of aquatic bacteria. This procedure, presented in several places (Hobbie et al. 1977; Standard Methods, 17th ed., 1989), involves sample fixation, staining with acridine orange, and counting with an epifluorescence microscope. DOC was determined by passing the sample through a 0.45 um filter, then measuring TOC with an O.I. Model 700 TOC Analyzer.

5.2 Results and Discussion

The raw data from this experiment are plotted in Figure 5.1. There was an initial lag period, during which no degradation and little growth were seen, followed by rapid growth and a corresponding decrease in TOC. The bacterial numbers reached a peak, then decreased as the readily degradable substrate became exhausted. After 6 days about 15 percent of the initial DOC had been removed.

The raw data were transformed for use in parameter estimation. The bacterial numbers were converted to mg Cell-Carbon/L using a factor of 2E-10 mg/cell (Gaudy & Gaudy, 1980), and the typical bacterial formula $C_5H_7O_2N$ (60mg C/113 mg biomass).

Manipulation of the DOC data was also necessary to obtain the biodegradable NOM. The non-biodegradable DOC was

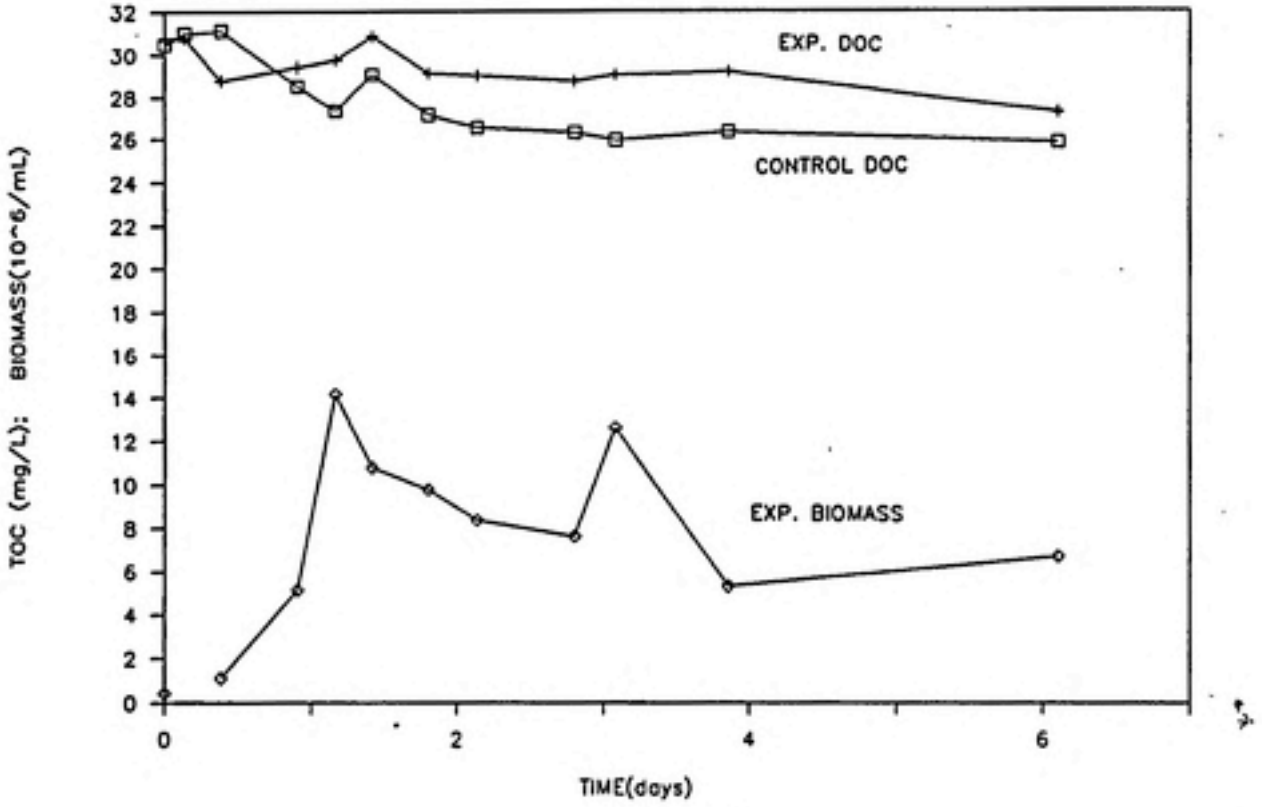

Figure 5.1 Raw DOC and Cell Number Data for Batch Biokinetic Experiment.

taken as that remaining after 2.8 days. Subtracting the non-biodegradable fraction (26.3 mg/L) from the initial DOC (31 mg/L) gave a biodegradable fraction of nearly 5 mg/L. The biodegradable fraction remaining at any time was calculated by subtracting the non-biodegradable fraction from the measured DOC. The manipulated data are plotted in Figure 5.2 as a function of time, which was adjusted by the lag period suggested in Figure 5.1. One outlier value of biodegradable DOC is indicated at time 1.0 day. This sample had not been filtered like the rest, so the biomass carbon (from the cell count data) was subtracted from the TOC to yield DOC. The adjusted DOC was 1.8 mg/L instead of 3.0 mg/L as measured. The data plotted in Figure 5.2 are also shown in Table 5.1.

Table 5.1 Manipulated Biokinetic Data used for Parameter Estimation

Time (days)	Biodegradable DOC (mg/L)	Cell-Carbon (mg/L)
0.0	4.8	0.1
0.5	2.2	0.5
0.8	1.0	1.5
1.0	1.6	1.1
1.4	0.8	1.0
1.8	0.2	0.9
2.4	0.0	0.8

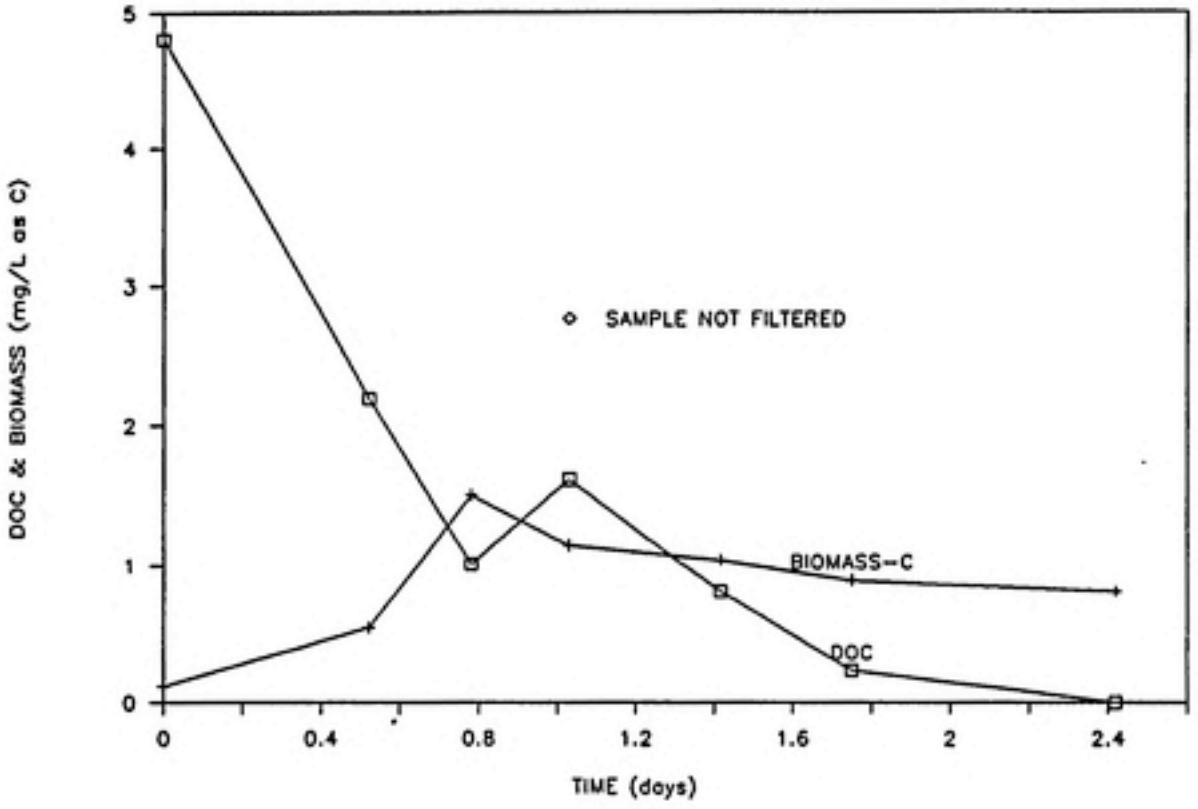

Figure 5.2 DOC of Biodegradable Fraction of NOM and Cell Carbon Data for Batch Biokinetic Experiment.

5.3 Estimation of Parameters

5.3.a Monod Model

An attempt was made to fit Monod biokinetic parameters to the data using nonlinear regression, using Equations 5.1 and 5.2.

$$dS/dt = -(k_m*S*X)/(K_s+S) \qquad (5.1)$$

where:

dS/dt = Rate of substrate utilization (mg/L-d)

k_m = Max specific substrate utilization rate (hr-1)

S = Substrate (TOC) concentration (mg/L)

X = Avg. biomass concentration (mg/L as C)

K_s = Half velocity constant (mg/L)

$$dX/dt = Y*(k_m*S*X)/(K_s+S) - k_d*X \qquad (5.2)$$

where:

dX/dt = Rate of biomass growth (mg/L-d)

Y = Yield coefficient (mg Cell-C/mg TOC)

Attempts to fit the Monod model to these data were unsuccessful. This was due to an insufficient number of experimental data.

Other researchers have determined Monod parameters for NOM. Hubele (1985) reported a u_m of 0.65 hr^{-1} and a K_s

value of 1.64 mg/L. Werner and Hambsch (1986) reported a u_m of 0.61 hr^{-1} and a K_s of 7.7 mg/L. It is not possible to compare these values with any parameter values presented in this report, because it was not specified whether the u_m and K_s values referred only to the biodegradable fraction of the NOM, or to the total NOM in solution.

5.3.b First-Order Model

Since the Monod model could not be fitted to these data, a first order (with respect to substrate concentration) model was used. The equation used for the rate of substrate utilization was:

$$dS/dt = -k*S*X \qquad (5.3)$$

where: dS/dt = rate of substrate utilization (mg/L/d)

k = first order rate constant (L/mg Cell-C/d)

This equation was integrated to yield the equation:

$$\ln(S) = \ln(S_0) - k*X*(t-t_0) \qquad (5.4)$$

where:

S = DOC concentration at time t (mg/L)

S_0 = Initial DOC concentration (mg/L)

The use of this equation for determining k requires that the biomass concentration, X, be relatively constant during the course of the experiment. Since the biomass concentration was not constant, this equation was evaluated over each time interval, using the average biomass concentration for that interval. The resulting equation is shown below:

$$\ln(S_i) = \ln(S_{i-1}) - k*(X_{i-1}+X_i)/2*(t_i-t_{i-1}) \qquad (5.5)$$

where:

S_i = DOC at time i (mg/L)

S_{i-1} = DOC at time i-1 (mg/L)

X_i = Biomass concentration at time i (mg/L as C)

X_{i-1} = Biomass concentration at time i-1 (mg/L as C)

t = time (hrs)

This equation was solved for k, and used to calculate k for each interval. The equation used was:

$$k = -\ln(S_i/S_{i-1})/((X_{i-1}+X_i)*(t_i-t_{i-1})/2) \qquad (5.6)$$

The data for each interval, plus the corresponding values of k are shown in Table 5.2. The average value of k was 3.2 L/mg cell-C/day.

Table 5.2 Data For Determination of First-Order Biokinetic Rate Constant

i	S_{i-1} (mg/L)	S_i (mg/L)	X_{avg} (mg/L)	k (L/mg/d)
1	4.8	2.2	0.3	5.2
2	2.2	1.0	1.0	2.6
3	1.0	1.6	1.3	---
4	1.6	0.8	1.0	1.7
5	0.8	0.2	1.0	3.5
6	0.2	0.0	0.8	---

Biomass growth was modeled to estimate Y and K_d using Equation 5.7.

$$dX/dt = Y*k*S*X - K_d*X \qquad (5.7)$$

where:

dX/dt = Rate of Cell-C production (mg/L/d)

Y = Yield coefficient (mg/mg)

k = first order rate constant (L/mg/d)

K_d = Coefficient of decay (day-1)

For this analysis, each interval was again treated separately, using an average substrate (DOC) concentration

for each interval. The equation was integrated to yield:

$$\ln(X_i/X_{i-1}) = (YkS_{avg} - k_d)*(t_i - t_{i-1}) \qquad (5.8)$$

Solving for the term $(YkS_{avg} - k_d)$ gives:

$$(YkS_{avg} - k_d) = \ln(X_i/X_{i-1})/(t_i - t_{i-1}) \qquad (5.9)$$

The value of $(YkS_{avg} - k_d)$ was calculated for each interval, and is shown in Table 5.3. This term, a linear function of S_{avg}, is shown plotted versus S_{avg} in Figure 5.3. Linear regression performed on the data yielded values of Y and k_d of 0.37 mg Cell-C/mg DOC consumed and 0.86 day-1, respectively.

Table 5.3 Data For Determination of Yield Coefficient and Coefficient of Microbial Decay.

i	X_{i-1} (mg/L)	X_i (mg/L)	S_{avg} (mg/L)	(t_i-t_{i-1}) (days)	$(YkS_{avg}-k_d)$ (day^{-1})
1	0.1	0.5	3.5	0.5	3.2
2	0.5	1.5	1.6	0.3	3.7
3	1.5	1.1	1.3	0.2	-1.6
4	1.1	1.0	1.2	0.4	-0.2
5	1.0	0.9	0.5	0.4	-0.3
6	0.9	0.8	0.1	0.6	-0.2

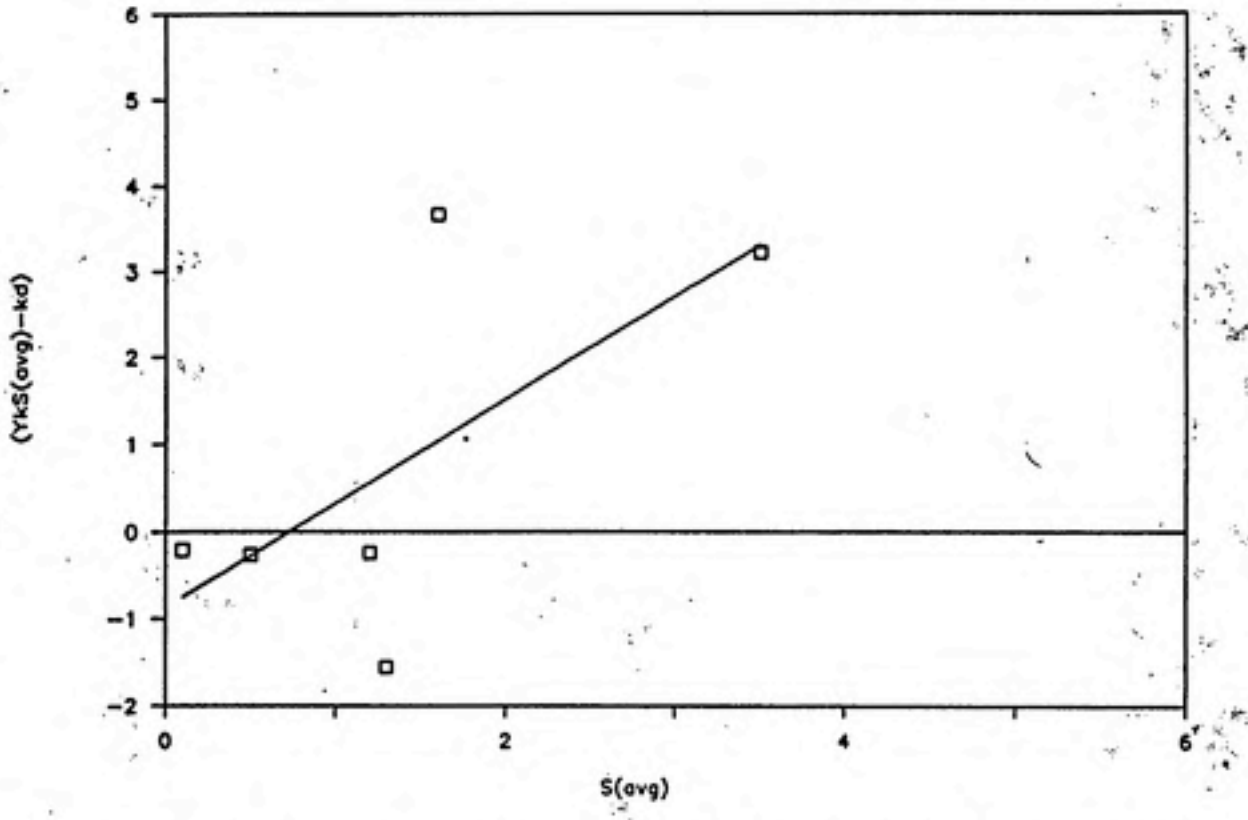

Figure 5.3 Linear Regression For Determination of Y and k_d.

The values of k, Y, and k_d obtained from the first-order model were used to integrate the dS/dt and dX/dt functions simultaneously, using the TUTSIM (Applied i, Palo Alto, California) integration package. In addition to k,Y, and k_d, the integration required the initial DOC and biomass concentrations. The TUTSIM results, along with the experimental data points are shown in Figure 5.4. These parameters produced a satisfactory fit, despite the small number of data collected. A summary of the first-order biokinetic parameters for each biodegradable component of the NOM solution is given in Table 5.4.

Table 5.4 Summary of First-Order Biokinetic Parameters

PARAMETER	VALUE	DESCRIPTION
k	3.2	1st-order constant (L/mg Cell-C/d)
Y	0.37	Yield coefficient (mg Cell-C/mg DOC)
k_d	0.86	Coeff. of microbial decay (day-1)

5.3.c Biokinetic Parameters for Model NOM Solutions

The Multicomponent Adsorption and Biodegradation (MCAB) model, discussed in Chapter 8, models the biodegradation of NOM according to Monod kinetics. Therefore, Monod biokinetic parameters were derived which forced the Monod

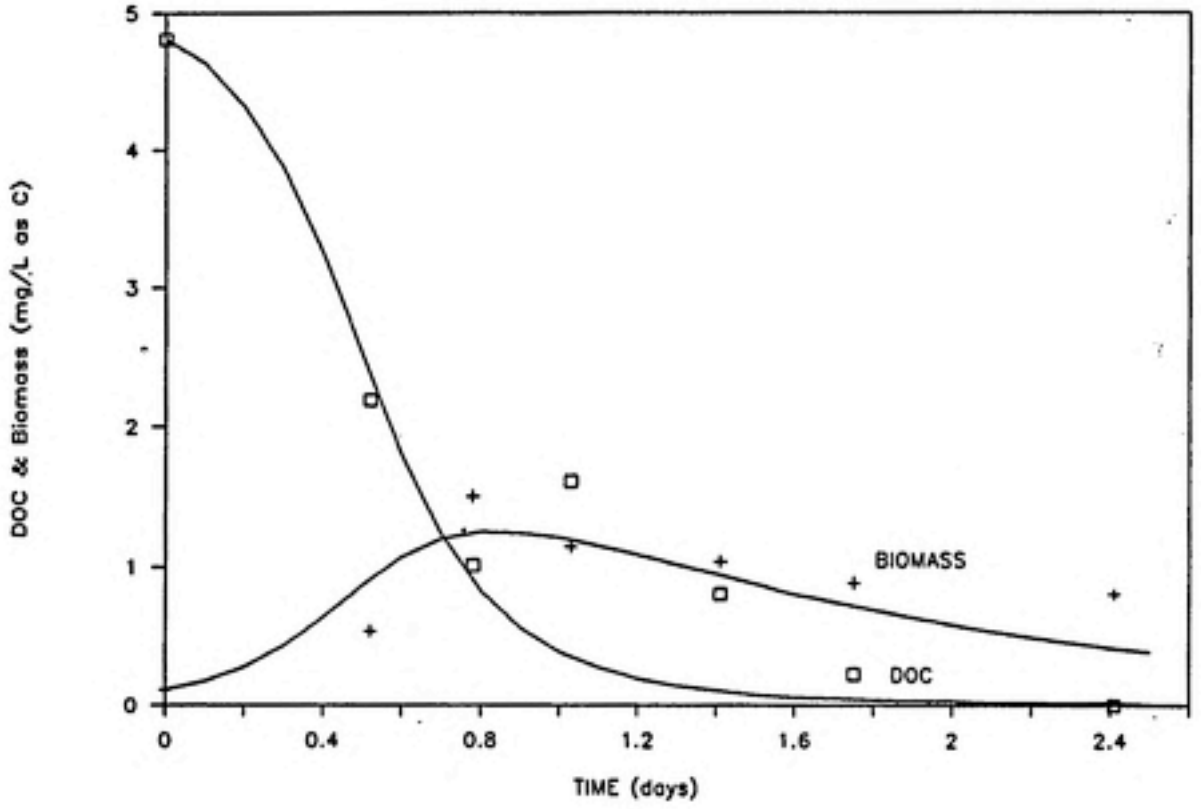

Figure 5.4 Results of First-Order Model Used to Simulate Results of Batch Biokinetic Study.

equation to approximate first-order kinetics. The rate of substrate utilization is given by Equation 5.10.

$$dS/dT = -(k_m*S*X)/(K_s+S) \qquad (5.10)$$

When K_s is much greater than S, the S in the denominator is negligible, and the equation becomes:

$$dS/dT = -(k_m/K_s)*S*X \qquad (5.11)$$

Equation 5.10 is a first-order substrate utilization expression, with the quotient k_m/K_s equivalent to the first-order rate constant k in Eq. 5.2. In this case, the values of k_m and K_s are unimportant, so long as the quotient equals k, or 3.2 L/mg Cell-C/day. The values of k_m and K_s were determined such that the value of the Monod expression (Eq. 5.9) changed no more than one percent over the range of possible TOC concentrations (0.0 to 17.7 mg/L). The calculated values of k_m and K_s were 228 mg TOC/mg Cell-C/hr and 1752 mg/L, respectively. The parameter values for approximating first-order kinetics with the Monod equation are summarized in Table 5.5.

Table 5.5 Monod Biokinetic Parameters Used to Approximate First-Order Kinetics.

Parameter	Value
k_m	228 mg TOC/mg Cell-C/hr
K_s	1752 mg/L
Y	0.37 mg Cell-C/mg TOC consumed
k_d	0.86 day^{-1}

These parameters were used as input to the MCAB model for the biodegradable components of the model NOM solution. It should be noted, however, that the values of k_m and K_s calculated for use in the model are much too high to be considered realistic, and that they are only useful for approximation of first-order kinetics with the Monod equation.

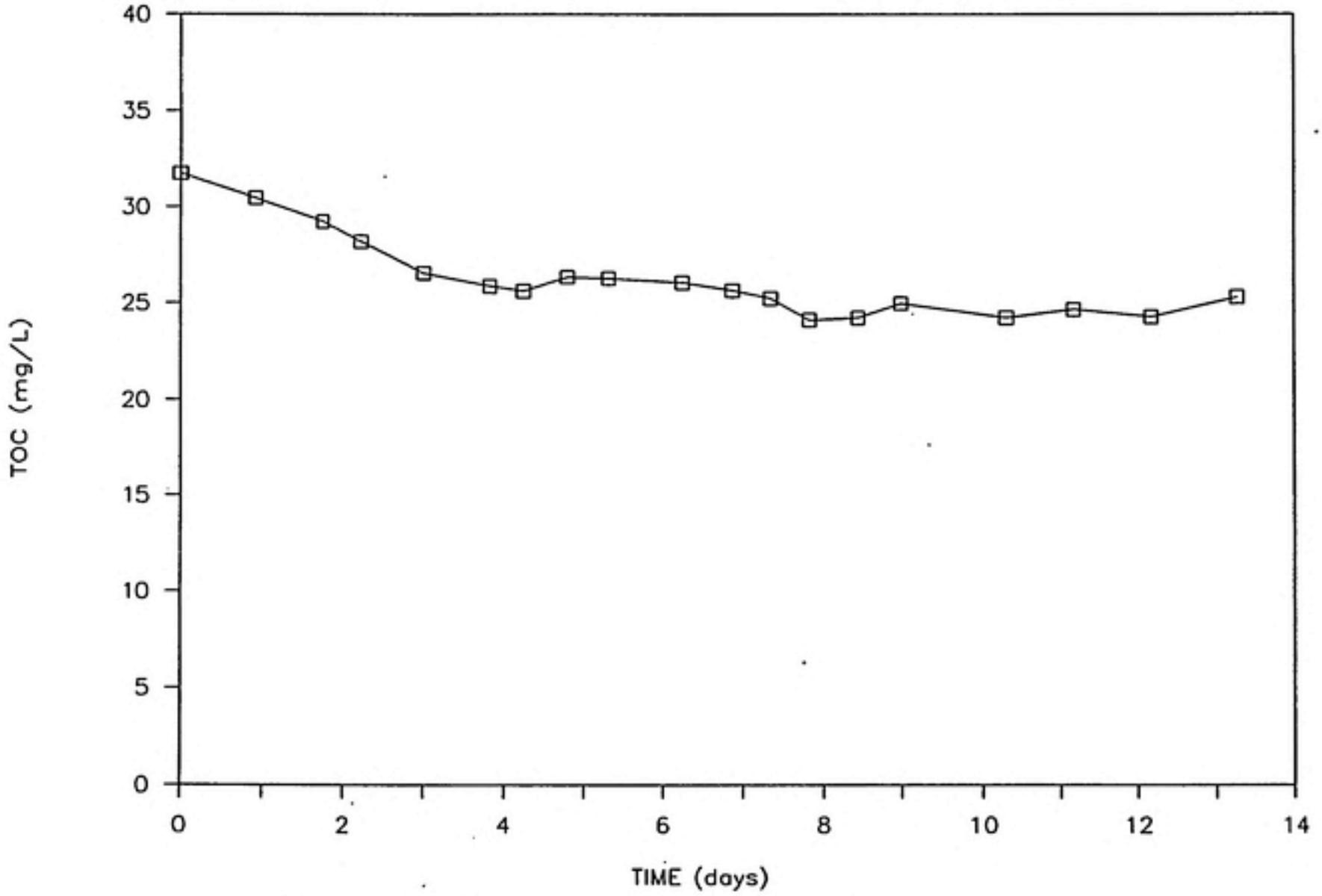

Figure 6.2 Biostabilization of Ozonated NOM in Batch Recycle Reactor.

of NOM in a continuous flow recycle reactor containing GAC. The continuous flow reactor, designed for the study of adsorption-biodegradation interactions, is described in Section 6.3. The important observation, with regard to this research, was that with an EBCT of 3.8 minutes, the continuous flow reactor achieved a steady-state TOC removal greater than 40 percent using the same ozonated NOM as in the batch reactor. In contrast, only 22 percent TOC removal was accomplished in the batch reactor.

One possible explanation for less biodegradation in the batch-recycle reactor relates to NOM heterogeneity. The composition of the substrate to which the microorganisms in a reactor are exposed may be important. In the batch recycle reactor, the composition of the NOM changes with time, with the most easily degraded fractions the first to be consumed. Once these are gone, only the more recalcitrant fractions remain, which are less energetically profitable for the microorganisms. This depletion of the readily degradable fractions could lead to stress of the microbial population, as it is forced to adapt to the new composition. After a few iterations of consumption and adaptation, the microorganisms reach a point where they can degrade no more of the NOM.

The continuous flow recycle reactor is intended to simulate a differential element of GAC by internal recycle of the effluent at a high rate. Due to the high recycle ratio used in the differential reactor, the microbial

population is exposed to all of the various fractions continuously. Because the composition of the feed to the reactor (i.e., influent plus recycle) varies little with time, the microbial population may be viewed as fairly stable. Thus, the microbial community in this reactor configuration may have an inherent advantage over the microbial population in the batch-recycle reactor. Another possible explanation for higher steady-state removal of TOC in the continuous flow recycle reactor is the use of GAC rather than anthracite as the bacterial attachment media. It has also been suggested that slow adsorption kinetics, in addition to biodegradation, may be responsible for long term low level DOC removal and extended GAC bed life (Neukrug et al., 1984; Maloney et al., 1984). Therefore, the removal attributed to biodegradation may, in fact, be overestimated if adsorption also takes place at steady-state.

6.3 Biodegradation on GAC Versus Anthracite

As a result of the apparently incomplete stabilization of the ozonated NOM in the recycling batch reactor, the continuous flow recycle reactor was chosen to accomplish the biostabilization of the sample. The strategy was to allow the reactor to reach steady state then increase the empty bed contact time (EBCT), and repeat - in an iterative fashion - until no additional decrease in TOC could be seen. In addition, to ensure that the observed difference in

performance between the reactors was due to their configurations, and not to differences in media, one reactor was filled with GAC and another with anthracite. These reactors were run in parallel (both continuous flow with recycle).

A schematic diagram of the continuous flow system, which was designed for adsorption and biodegradation of natural organic material by DeWaters (DeWaters, 1987), is presented in Figure 6.3. The system features a glass fixed bed column with a bed volume of 5.38 cm^3, which holds approximately 4 grams of GAC. A complete description of the reactor system components is given elsewhere (DeWaters 1987). A high recycle ratio was used, which provided differential reactor operation. A differential reactor is one in which there is only a small change in concentration across the bed, and a potentially large difference between the feed and effluent concentrations. This is possible because the feed solution is substantially diluted by the recycled reactor effluent, and enters the reactor at a concentration only slightly higher than the effluent concentration. This mode of operation, which approaches CSTR performance, minimizes both the concentration gradient across the bed, and the effect of axial position on kinetics.

The operating conditions for both reactors are summarized in Table 6.1. EBCT is defined by the flow rate

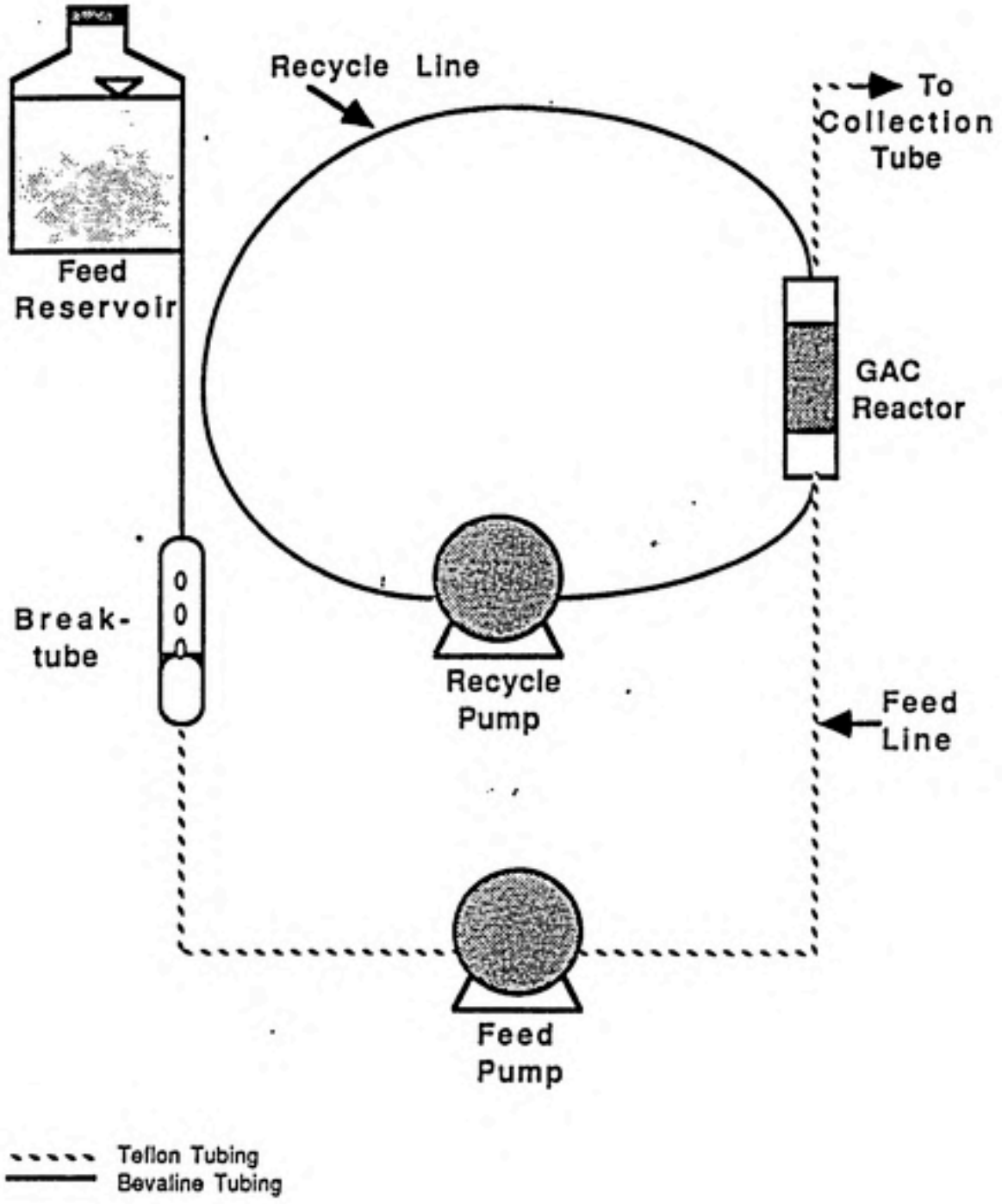

Figure 6.3 Schematic of Continuous Flow Recycle Reactor (from DeWaters, 1987).

to the reactor and the volume of the reactor:

$$EBCT = V_R/Q \quad (6.1)$$

where:

V_R = Volume of reactor (cm^3)

Q = Feed flowrate (cm^3/min)

The added flowrate due to recycle is used to calculate the per pass contact time (PPCT), as given by Equation 6.2.

$$PPCT = V_R/(Q + Q_R) \quad (6.2)$$

where:

Q_R = Recycle flowrate (cm^3/min)

TABLE 6.1 Summary of Operating Conditions for Continuous Flow Recycle Reactors

INTERVAL (days)	FLOW (L/d)	RECYCLE FLOW (L/d)	GAC REACTOR EBCT (min)	GAC REACTOR PPCT[1] (min)	ANTHRACITE REACTOR EBCT (min)	ANTHRACITE REACTOR PPCT[1] (min)
1-13	2.0	72	3.8	0.1	3.8	0.1
13-25	0.3[2]	72	25.6	0.1	25.6	0.1
25-33	0.3[2,3]	72	51.2[3]	0.1	25.6	0.1

1. Per pass contact time.
2. Anthracite reactor fed Deionized water plus nutrients
3. Previously collected GAC reactor reactor effluent fed to GAC reactor to double longest EBCT.

The initial feed rate to each reactor was 2.0 L/day, which resulted in an EBCT of 3.8 minutes. On day 12, the EBCT in each reactor was increased to 25.6 minutes. On day 25, the EBCT of the GAC reactor was increased to 51.2 minutes. The changes in EBCT and feed solutions are discussed in a later section. The recycle rate, held constant throughout the experiment, was 50 mL/min (72 L/day). This high recycle rate maintained the per pass contact time (PPCT) approximately constant at 0.1 minutes, despite changes in the feed rate.

The feed solution was prepared by diluting ozonated lake water to a TOC of about 18 mg/L, buffering to a pH of 6.5, and adding nutrients as before. Prior to start-up, 1.0 mL of a bacterial seed solution was added to the inlet end of each reactor. The bacterial seed was prepared by adding a 50 mL volume of ozonated lake water to 50 mL of non-ozonated water, and allowing the mixture to incubate at room temperature for 24 hours.

The effluent TOC and TIC concentration profiles of both reactors through Day 6 are shown in Figure 6.4. The pattern of TOC removal in the GAC reactor was similar to that observed by DeWaters. The breakthrough pattern observed by DeWaters, shown in Figure 6.5, is characterized by a typical breakthrough early in the run, followed by a dip in the effluent concentration and a more gradual breakthrough, until sorptive capacity is exhausted and a steady state effluent concentration is reached. The effluent TOC

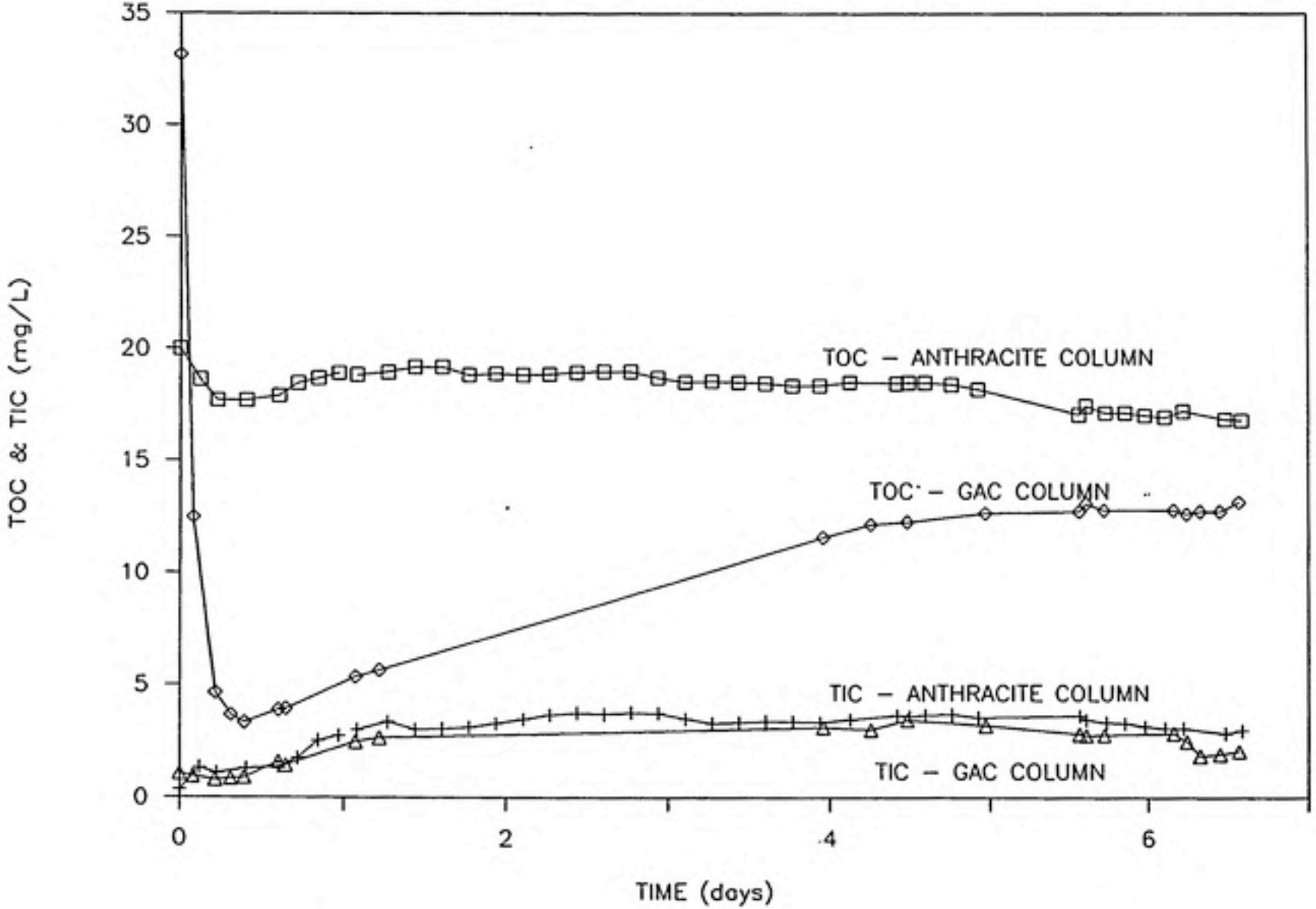

Figure 6.4 GAC and Anthracite Continuous Flow Recycle Reactor Results.

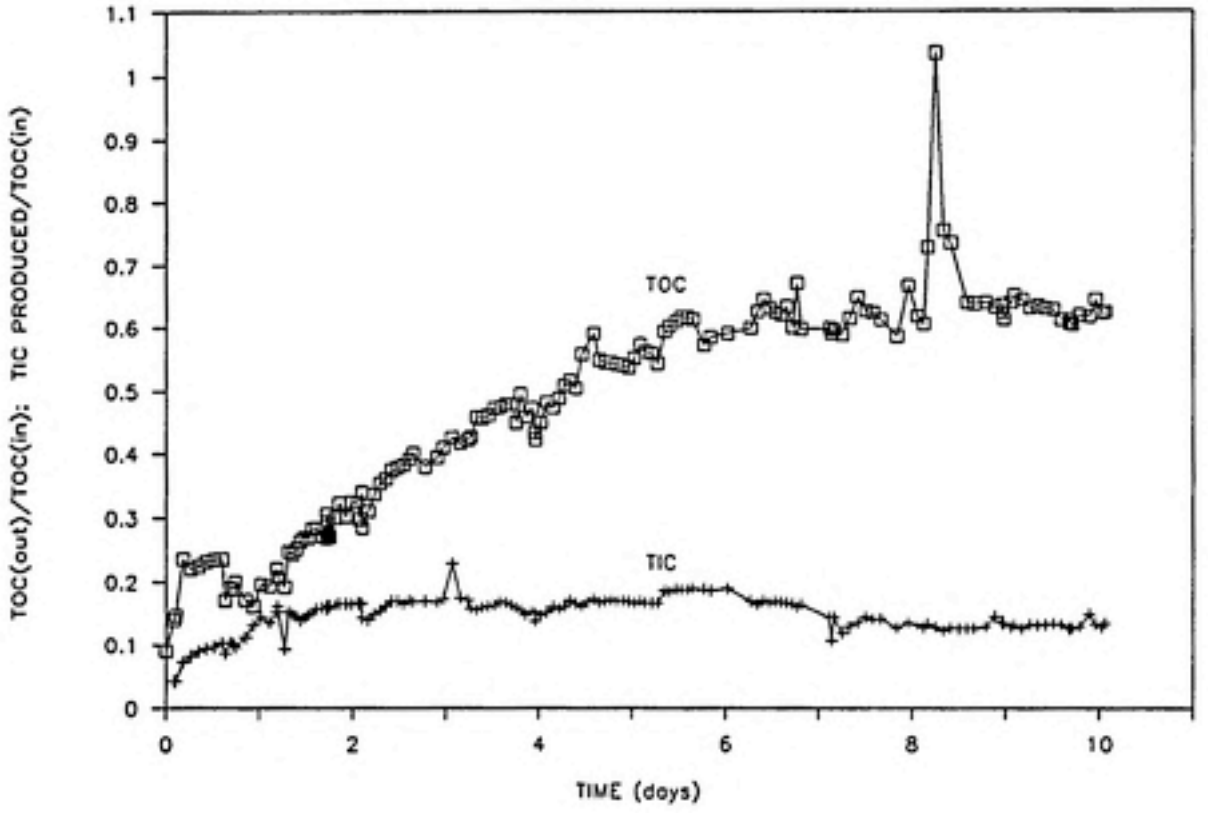

Figure 6.5 TOC Breakthrough and CO_2 Production for Continuous Flow Recycle Reactor with GAC Media (DeWaters, 1987).

concentration does not rise to the level of the feed concentration, which suggests biodegradation is responsible for steady-state removal. The spike of TOC in the GAC reactor effluent (Figure 6.4), possibly due to wash out of GAC fines, obscured the early section of the breakthrough curve in this experiment. After about six days, the GAC column showed a 28 percent reduction in TOC, whereas the anthracite column had accomplished little TOC removal. This difference could be attributed to the fact that GAC adsorbs TOC, whereas anthracite does not. However, biological activity was suspected to occur in both reactors, as evidenced by the increase in TIC, presumably due to microbial CO_2 production. Therefore, TOC removals should have been expected in both reactors due to biodegradation.

The fact that TIC increased through the anthracite reactor but TOC was not removed suggests either that anthracite itself served as a substrate or that TIC was being abiotically produced. To resolve this question, the feed solution to the anthracite column was replaced with distilled deionized (DDI) water, with the usual buffering and nutrients on Day 18 of the experiment. The influent and effluent TOC and TIC concentrations for the anthracite column are shown in Figure 6.6. This change in feed resulted in an immediate drop in effluent TOC, as expected, but produced very little change in the effluent TIC. The results of the anthracite reactor are summarized in Table 6.2.

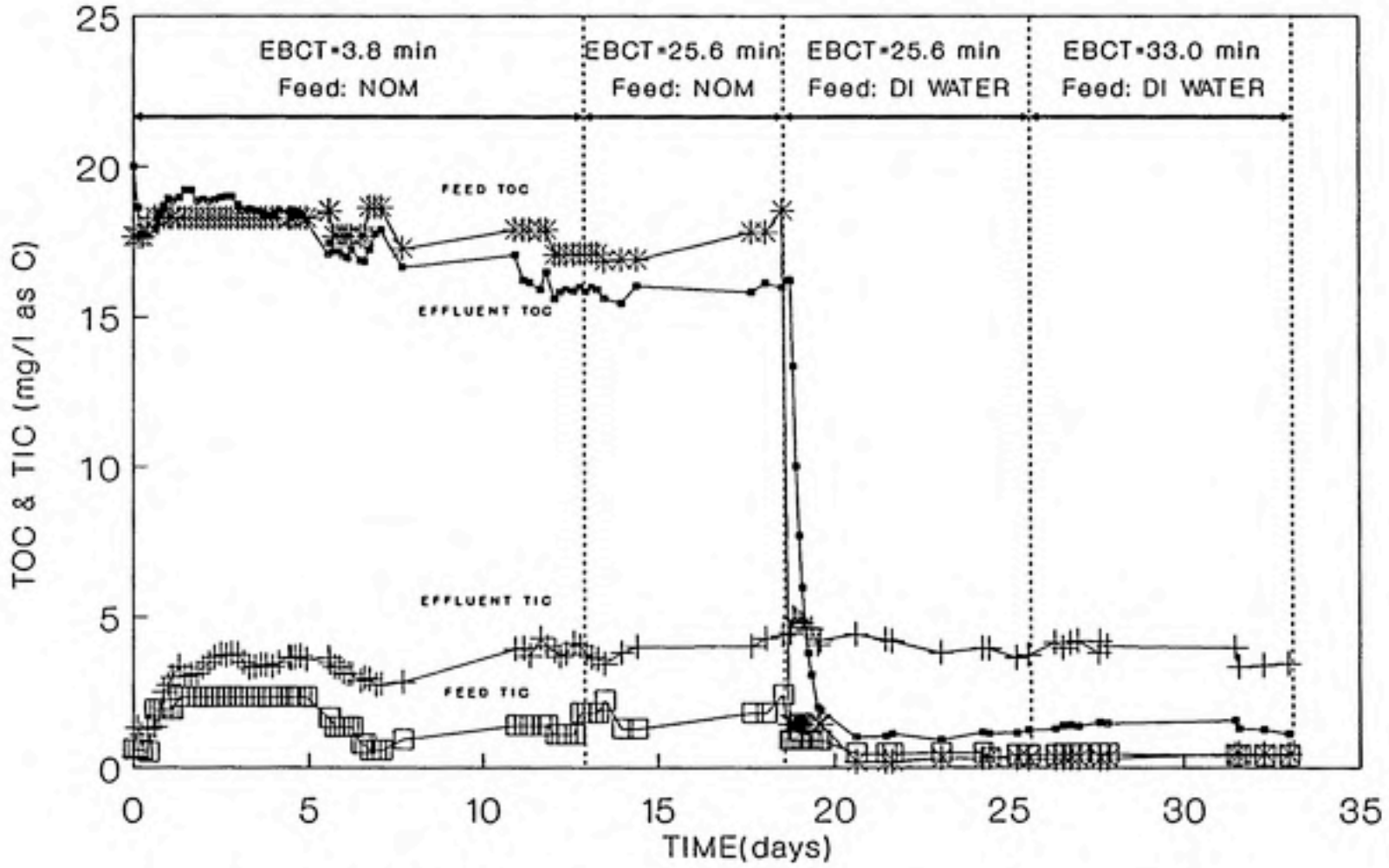

Figure 6.6 TOC Breakthrough and CO_2 Production for Continuous Flow Recycle Reactor with Anthracite Media.

TABLE 6.2 SUMMARY OF ANTHRACITE REACTOR PERFORMANCE

INTERVAL (days)	FEED SOLUTION	EBCT (min)	TOC REMOVED (mg/L)	TIC PRODUCED (mg/L)
1-13	NOM	3.8	0.2	1.5
13-18	NOM	25.6	1.4	2.1
18-33	DI H_2O	25.6	-1.0	3.5

TIC production during all three periods exceeded the amount of carbon which could be accounted for by a decrease in TOC. This, in addition to the fact that the TIC production was at a maximum when no NOM was being fed to the reactor, served to confirm that the TIC production was not due to biodegradation of NOM. Some other explanation, therefore, is needed for the observed TIC production. Certain fungi have been shown capable of degrading anthracite coal (Scott and Strandberg, 1986). While anthracite coal could have served as a carbon source for the microorganisms, this seems unlikely when a much more readily degradable substrate (ozonated NOM) was available. Another possibility is that CO_2 was produced by a reaction between the water and anthracite.

No simple explanation could be given for the lack of biological activity in the anthracite reactor. In contrast, the plateau in TOC removal achieved in the GAC reactor was good evidence of biodegradation. Thus, the decision was made to use the GAC reactor to obtain a biostabilized

sample. This assumes that the plateau in TOC removal after six days of operation is solely due to biodegradation, and not to slow adsorption, as has been postulated by Maloney et al. (1984).

The TIC and TOC for the influent and effluent of the GAC column are shown in Figure 6.7. Once the longest EBCT had been reached (day 23), about 3 L of the effluent was collected and used as influent to the reactor. This was done to double the longest EBCT used, giving a total EBCT of 51 minutes. The resulting effluent was considered to be biostabilized. The results of the GAC reactor are summarized in Table 6.3.

TABLE 6.3 SUMMARY OF GAC REACTOR PERFORMANCE

INTERVAL (days)	FEED SOLUTION	EBCT (min)	TOC REMOVED (mg/L)	TIC PRODUCED (mg/L)	YIELD	TOC REMOVAL (%)
1-13	NOM	3.8	5.5	1.9	0.65	34
13-25	NOM	25.6	8.4	2.5	0.70	48
25-33	effluent	51.2	10.4	2.9	0.70	55

The degree of TOC removal was 31 percent for the shortest EBCT (3.8 min.), and reached 55 percent at the longest (51.2 min.). Therefore, the biodegradable fraction of the ozonated NOM was considered to be 55 percent, for the modeling discussed in Chapter 8. The non-biodegradable

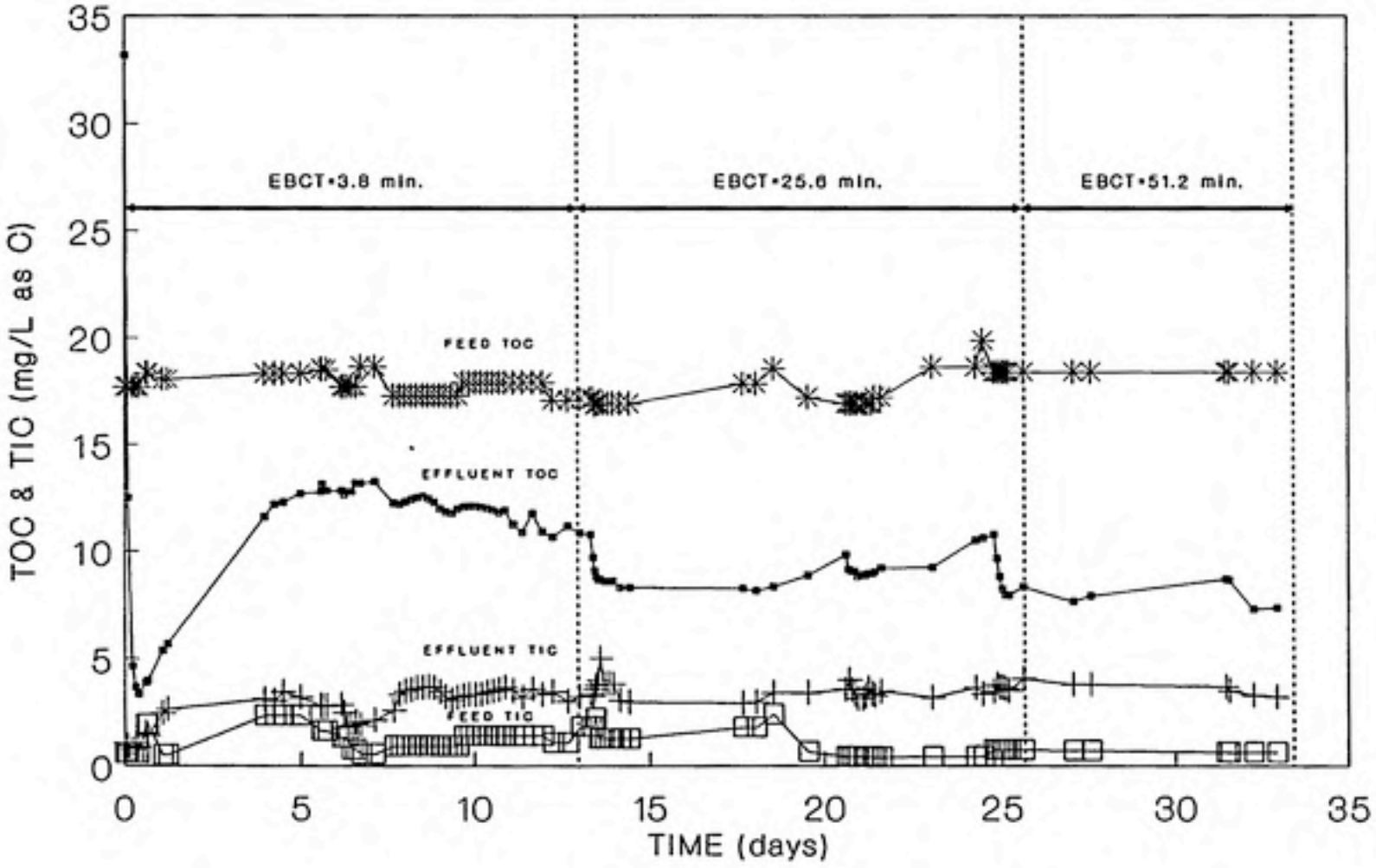

Figure 6.7 TOC Breakthrough and CO_2 Production for Continuous Flow Recycle Reactor with GAC Media.

fraction is that which remains following biostabilization, or 45 percent. The yield values calculated for the various intervals range from 0.65 to 0.70 (mg Cell-C/mg TOC consumed). These values are lower than the value of 0.8 reported by DeWaters (1987).

To estimate whether the long term steady-state TOC removal could be due to adsorption rather than biodegradation, the time necessary for exhaustion of the adsorption capacity was calculated using a simple equilibrium model. The adsorption capacity of the GAC was determined from the ozonated NOM isotherm presented in Chapter 7. The equilibrium mass loading corresponding to an equilibrium liquid phase TOC concentration of 17.7 mg/L is 13.8 mg/g. Breakthrough time was calculated using the assumption of equilibrium adsorption in the GAC bed, with no mass transfer limitations. This gave:

$$t_B = (W*q)/(Q*C_0) \qquad (6.3)$$

$$= (4 * 13.8)/(2 * 17.7) = 1.6 \text{ days}$$

where:

t_B = breakthrough time (days)

W = mass of GAC in reactor (g)

Q = feed flow rate (L/d)

C_0 = TOC concentration in feed (mg/L)

q = equilibrium mass loading at C_0 (mg/g)

The estimated breakthrough time of 1.6 days is shorter than the operating time of the GAC bed before steady-state was

reached (about 6 days). It is impossible to state, without detailed mathematical modeling, that mass transfer limitations of external and internal diffusion would not lengthen the breakthrough time by a factor of 3.8 (6 days/1.6 days). Since the sample of biostabilized NOM was collected between Day 25 and Day 28, adsorption was thought to be insignificant. Nevertheless, it cannot be dismissed as a possible mechanism for TOC removal.

CHAPTER 7. DETERMINATION OF ADSORPTION PARAMETERS

7.1 Experimental Method

Adsorption isotherms were determined for ozonated NOM and ozonated-biostabilized NOM using the bottle point method (Randtke and Snoeyink, 1983). The constant C_0 (initial adsorbate concentration) approach was used, wherein the initial volume and adsorbate concentration (NOM) were constant from bottle to bottle, and the mass of adsorbent (powdered activated carbon, or PAC) was varied. This approach was favored over the constant adsorbent dose approach in which the mass of PAC added to each bottle is the same, and the concentration of the solution is different. For a solution containing one adsorbate, the two approaches will yield the same adsorption isotherm. However, when more than one adsorbate is present, which is envisioned because NOM is a heterogeneous substance, different adsorption isotherms are obtained (Harrington & DiGiano 1989).

Calgon F-400 (30/40 mesh) was ground to a mesh size of 200/325 (U.S. Standard Sieve Size) for the bottle point tests. PAC dosages ranging from 5 to 4000 mg/L were added to 20 bottles containing 100 mL of the NOM solution buffered

to pH 6.5. Two control bottles which contained no PAC were used for each isotherm. Following PAC addition the bottles were placed on a tumbler for a period of 10 days. An equilibration period of 7 days was found to be adequate for a NOM solution from Lake Drummond (Harrington and DiGiano, 1989). Biodegradation during equilibration was of special concern because ozonation has been shown to increase biodegradability of NOM (Hubele, 1985). In addition, sodium azide at a dosage of 5 mg/L had not been found effective in controlling biodegradation of ozonated NOM during 7 days of equilibration at a temperature of 23° C (Harrington and DiGiano, 1987). Therefore, equilibration was conducted at 4° C to minimize biodegradation of the ozonated NOM during the course of the experiment. At the end of the equilibration period, the contents of the bottles were passed through 0.45 um filters and analyzed for TOC. The mass loading (q) of TOC on the PAC was then calculated using the equation:

$$q_e = [(TOC)_0 - (TOC)_e] * (V/M) \qquad (7.1)$$

where:

q_e = Equilibrium TOC concentration in adsorbed phase (mg TOC/g PAC)

$(TOC)_0$ = Initial TOC concentration in bulk solution (mg/L)

$(TOC)_e$ = Equilibrium TOC concentration in bulk solution (mg/L)

M = Mass of PAC (g)

V = Volume of bulk solution (L)

7.2. Determination of Adsorption Isotherms for NOM Solutions

Adsorption isotherms for ozonated and ozonated-biostabilized NOM, both mixtures of unknown composition, were obtained using ideal adsorbed solution theory (IAST). IAST, developed by Myers and Prausnitz (1965) for modeling mixed gas adsorption, and later applied to multi-solute adsorption from dilute liquid solutions by Radke and Prausnitz (1972), contains the following assumptions: 1) the adsorbent phase is inert and has an identical surface area for all adsorbates; 2) the bulk liquid phase is a dilute solution that obeys Henry's law; and 3) the adsorbed phase is solvent free and forms an ideal solution that obeys Raoult's law, with solutes adsorbing simultaneously at constant temperatures and spreading pressures.

Frick and Sontheimer (1983) developed the pseudo-component approach for modeling an unknown mixture as a group of pseudo-components using IAST, in which each pseudo-component is representative of an actual fraction of the mixture having similar adsorbabilities. The equations for IAST using the pseudo-component approach are presented elsewhere (Crittenden, Luft, and Hand (1985); Harrington, DiGiano, and Fettig (1989)).

The results of the bottle point experiments provide the

input to the model, including the initial TOC concentration in the bulk solution, the measured equilibrium TOC concentration ($(TOC)_e$) in each bottle, and the equilibrium solid phase TOC concentration (q_e) in each bottle calculated from Equation 7.1. According to the method developed by Crittenden, Luft, and Hand (1985), the Freundlich adsorption parameters, K_i and $1/n_i$, in addition to the initial concentration of each component, C_{0i}, are found by solving the system of equations represented by Equation 7.2.

$$C_{0i} - [q_i*(M/V)] - [q_i/\sum_{j=1}^{N}(q_j)] *[\sum_{j=1}^{N}(n_j*q_j)/(n_i*K_i)]^{n_i} = 0$$

for i=1 to N (7.2)

where:

C_{0i} = Initial TOC conc. in bulk solution.

q = Equilibrium TOC conc. in adsorbed phase.

K = Freundlich K.

n = Freundlich n.

N = Number of adsorbable PCs.

This system of equations is for C_{0i}, K_i, and $1/n_i$ via non-linear regression such that the difference between the observed and calculated equilibrium liquid phase TOC concentrations is minimized. The function to minimize is

given by:

$$SSR = \sum_{i=1}^{m} [(C_{Ti,obs} - C_{Ti,calc})/\sigma_{ci}]^2 \qquad (7.3)$$

where:

SSR = Residual sum of squares.

$C_{Ti,obs}$ = Observed equilibrium TOC conc.

$C_{Ti,calc}$ = Calculated equilibrium TOC conc.

σ_{ci} = Standard deviation of $C_{Ti,obs}$.

m = Number of bottles used in experiment.

7.3 Equilibrium Adsorption Results

7.3.a Isotherm for Ozonated NOM

The first adsorption experiment was run with ozonated Lake Drummond water(1 mg O_3/mg TOC) which had not been biostabilized. The control bottles revealed no significant decrease in TOC over the 10 days of this isotherm study; this suggested that biological activity had been prevented. The initial TOC of the NOM solution, determined from the experimental data, was 5.8 mg/L.

An isotherm was fitted to the data using the IAST model, as discussed in the previous section. The data and the fitted isotherm are shown in Figure 7.1. The results of the IAST model indicate that the ozonated NOM may be described as a mixture of two adsorbable pseudo-components and one non-adsorbable pseudo-component. The residual sum

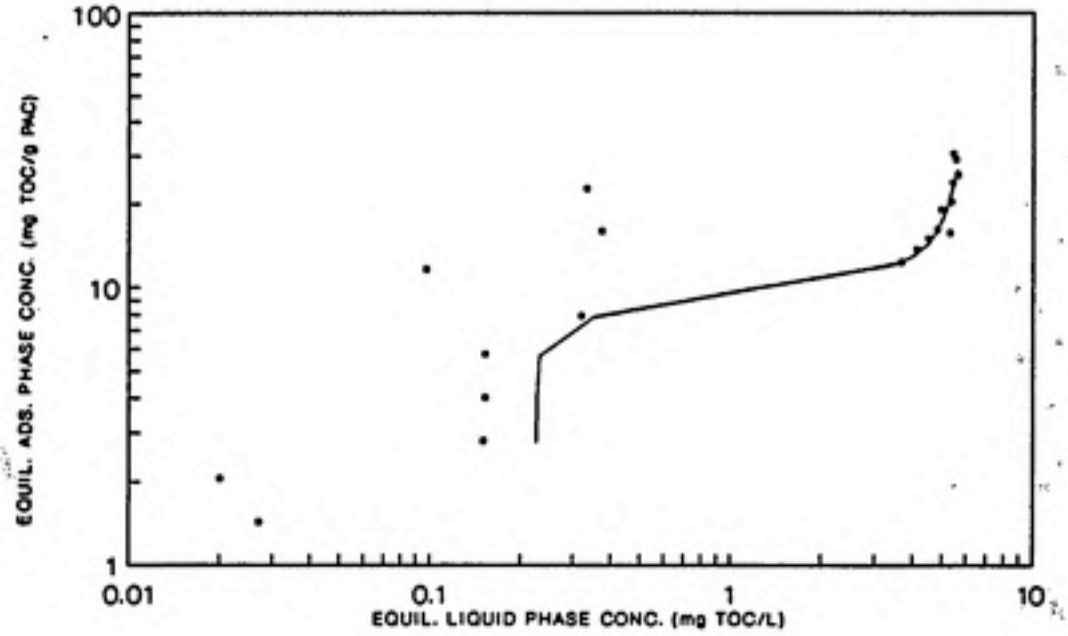

Figure 7.1 Equilibrium Adsorption Data and Fitted Isotherm for Ozonated NOM.

of squares (SSR), which is minimized during the curve fitting, is shown in Figure 7.2 as a function of the non-adsorbable concentration, C_{NA}. There is a pronounced dip when C_{NA} is four percent of the initial concentration, which gives the concentration of the solution's non-adsorbable fraction. This is similar to the findings of Summers and Roberts (1988), who reported a non-adsorbing concentration of not greater than three percent of the initial concentration, for aquatic humic and fulvic acid. The IAST model results for ozonated NOM are shown in Table 7.1.

Table 7.1. IAST Equilibrium Model Results for Ozonated NOM

Component	K	1/n	%C(T)
Pseudo-component 1	8.44	0.084	83
Pseudo-component 2	36.54	0.253	13
Non-adsorbing Pseudo-component	--	--	4

7.3.b Isotherm for Ozonated-Biostabilized NOM

Biostabilization of ozonated NOM was accomplished by running the NOM solution through a CSTR with an equivalent EBCT of 54 min, as described in Section 6.2. A bottle-point experiment was then performed on the ozonated-biostabilized NOM, as described in Section 7.1. Biodegradation of the ozonated-biostabilized sample during equilibration was not

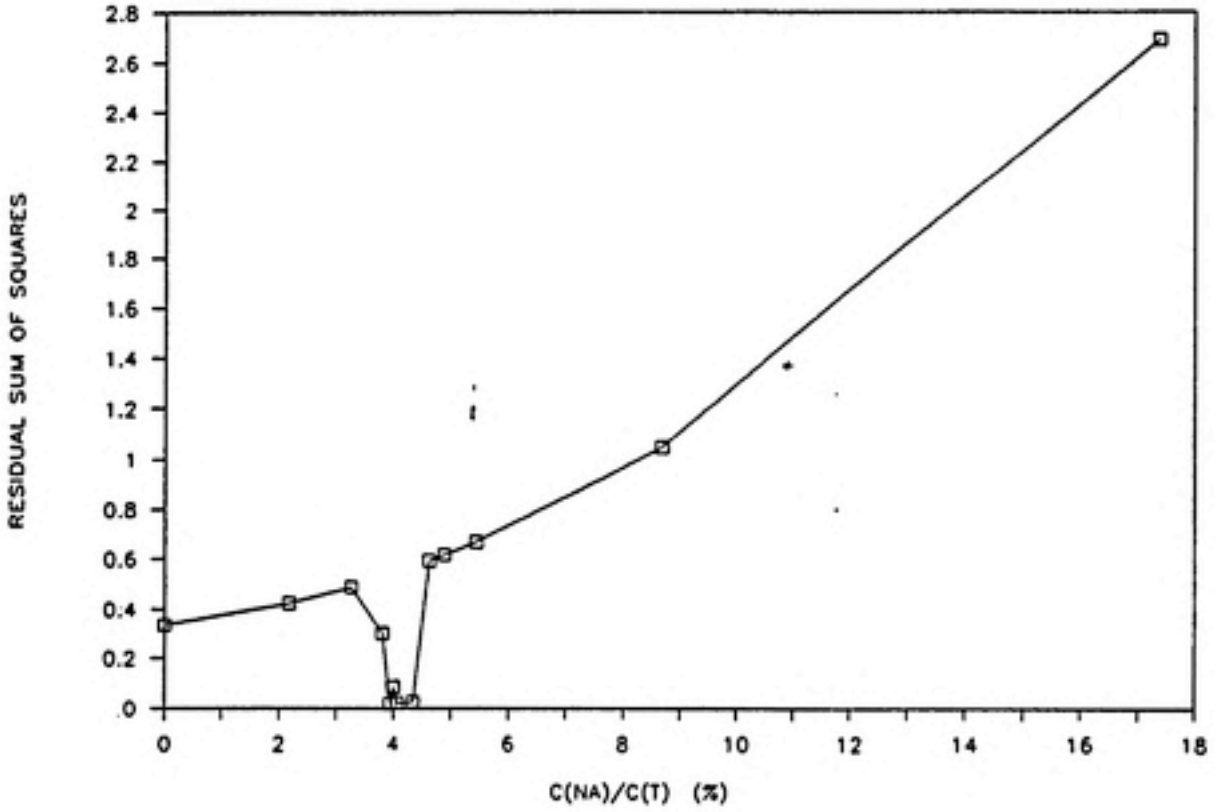

Figure 7.2 Residual Sum of Squares of Fitted Isotherm as a Function of Non-Adsorbable Fraction of Ozonated NOM.

of concern, because the NOM was already biostabilized. Nevertheless, this isotherm was measured at the same temperature (4^{o} C) as that for the ozonated NOM solution, to eliminate the confounding effect of temperature on comparison of the two isotherms. The control bottles containing NOM without activated carbon showed no decrease in TOC. The initial concentration of the NOM solution was 7.6 mg/L.

An isotherm was fitted to the data as before, to yield the concentrations and adsorption parameters of the pseudo-components. The data and the isotherm obtained for ozonated-biostabilized NOM are presented in Figure 7.3. As in the case of ozonated NOM, the ozonated-biostabilized NOM comprises two adsorbing pseudo-components. The SSR is shown versus C_{NA}/C_T in Figure 7.4. The minimum SSR occurs when C_{NA} is one percent of the initial concentration, but the corresponding decrease in the SSR is not significant. Therefore, a significant non-adsorbing pseudo-component is not thought to be present. These results indicate that most of the nonadsorbable fraction of the ozonated NOM was degraded during the process of biostabilization in the CSTR. This observation is supported by Hubele (1985), who reported that microorganisms preferentially utilize substrate with low carbon affinity. The term carbon used here denotes GAC. The IAST model results for ozonated-biostabilized NOM are shown in Table 7.2.

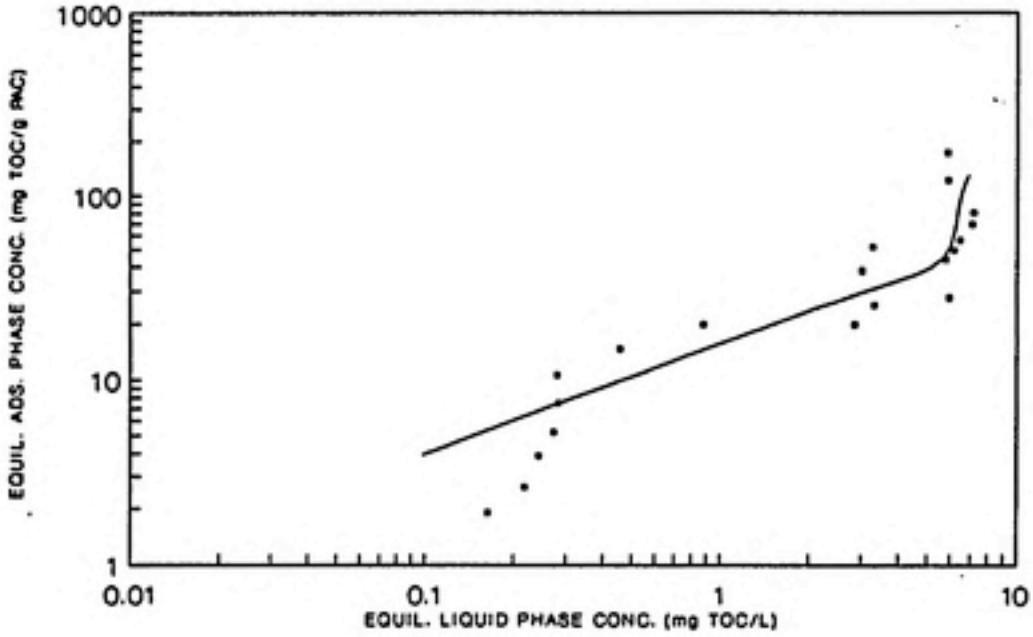

Figure 7.3 Equilibrium Adsorption Data and Fitted Isotherm for Ozonated-Biostabilized NOM.

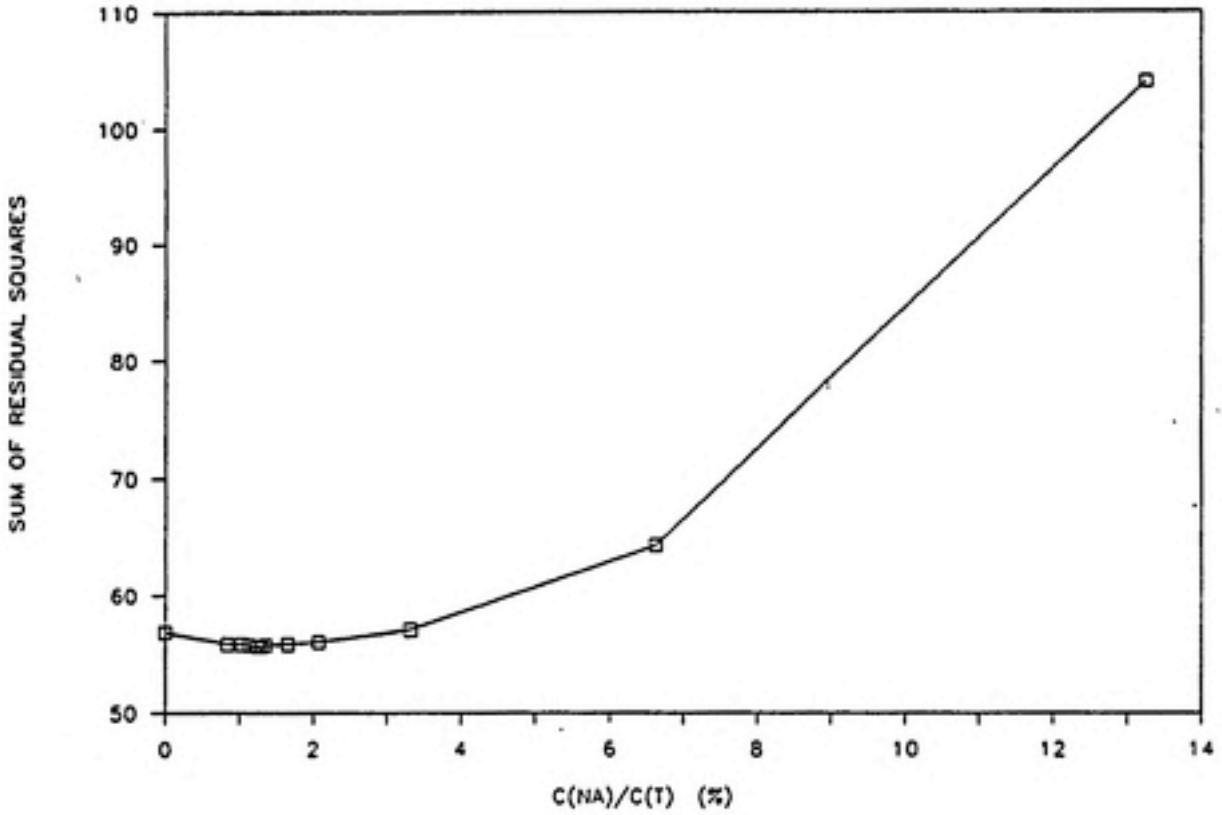

Figure 7.4 Residual Sum of Squares of Fitted Isotherm as a Function of Non-Adsorbable Fraction of Ozonated-Biostabilized NOM.

Table 7.2. IAST Equilibrium Model Results for Ozonated-Biostabilized NOM

Component	K	1/n	%C(T)
Pseudo-component 1	19.46	0.594	84
Pseudo-component 2	153.71	0.221	16

7.3.c Comparison of Ozonated and Ozonated-Biostabilized Isotherms

The relative concentrations of the adsorbable PCs changed little due to biostabilization. The concentration of PC No. 1 increased from 83 percent to 84 percent of the total concentration, and the concentration of PC No. 2 changed from 13 to 16 percent. This increase was offset by a decrease in the non-adsorbable fraction of four to zero percent of the total concentration. In contrast to the small changes in relative concentration, the adsorbability of both adsorbable PCs increased significantly.

Initially it is necessary to determine if the isotherm shapes differ because of differences in composition, or merely due to differences in solution concentration. Multicomponent isotherms can differ due to initial liquid phase concentration. Harrington and DiGiano (1989) showed that the position of isotherms for coagulated NOM depends upon initial concentration. A change in the composition of a mixture can also change its isotherm. Such a change is to

be expected, since biodegradation of a multisolute mixture produces a shift in the molecular weight distribution of the mixture, which is evidence of a change in the concentrations and/or other characteristics of the various components.

Once the Freundlich parameters and pseudo-component concentrations for a particular solution have been estimated by fitting an isotherm to the data, the IAST approach may be used to predict the isotherm at any concentration. This procedure was used to predict the isotherms for both ozonated NOM and ozonated-biostabilized NOM at the same initial concentration. An initial concentration of 7.0 mg/L was selected for the comparison. The predicted isotherms are presented in Figure 7.5. The two isotherms, predicted at the same concentration, show a difference in adsorbability, which is attributed to biological transformation of the ozonated NOM.

7.4 Implications for Modeling of NOM in the Recycle Reactor

7.4.a. Selection of Pseudo-Components for Model NOM Solution

The results of fitting isotherms to ozonated and ozonated-biostabilized NOM suggest that the relative concentrations of the adsorbable pseudo-components were

determined using the equation:

$$C_{B,T} = C_T * 0.55 \qquad (7.7)$$
$$= 17.7 * 0.55 = 9.7 \text{ mg/L}$$

Knowing from above that $C_{NA/B}$ is 7.0 mg/L, Equation 7.6 is satisfied if $C_{A/B}$ is 9.0 mg/L. $C_{A/B}$ is the sum of the adsorbable, biodegradable concentration of each adsorbable pseudo-component, and will be apportioned between the two adsorbable pseudo-components of the ozonated NOM later in this section.

3. DETERMINATION OF $C_{A/NB}$

$$C_{A,T} = C_{A/B} + C_{A/NB} \qquad (7.8)$$

The value of $C_{A,T}$ is obtained by:

$$C_{A,T} = C_T - C_{NA,T} \qquad (7.9)$$
$$= 17.7 - 0.7 = 17.0 \text{ mg/L}$$

Given that $C_{A/B}$ was found to be 9.0 mg/L, Equation 7.8 is satisfied if $C_{A/NB}$ is 8.0 mg/L. $C_{A/NB}$ is the sum of the adsorbable, non-biodegradable concentration of each adsorbable pseudo-component. This concentration will, like $C_{A/B}$, be divided between the two adsorbable pseudo-components of the ozonated NOM.

The above steps yield the following calculated composition of NOM:

$C_{A/B}$ = 9.0 mg/L

$C_{NA/B}$ = 0.7 mg/L

$C_{A/NB}$ = 8.0 mg/L

$C_{NA/NB}$ = 0.0 mg/L

The adsorbable fraction represented by $C_{A/B}$ and $C_{A/NB}$ must be distributed between the two adsorbable PCs of the ozonated NOM. The model results suggest that each of these PCs has a biodegradable fraction. Furthermore, the two adsorbing PCs were shown to have been biodegraded to approximately the same degree, as evidenced by the small change in their relative concentrations. For this reason, $C_{A/B}$ and $C_{A/NB}$ were distributed such that the biodegradable fraction of each PC was the same. The A/B and A/NB fractions ($f_{A/B}$ and $f_{A/NB}$) of the PCs were determined using Equations 7.10 and 7.11, respectively, and the concentrations calculated above.

$$f_{A/B} = (C_{A/B})/(C_{A/B} + C_{A/NB}) \qquad (7.10)$$

$$= 9.0/(9.0+8.0) = 0.53$$

$$f_{A/NB} = (C_{A/NB})/(C_{A/B} + C_{A/NB}) \qquad (7.11)$$

$$= 8.0/(9.0+8.0) = 0.47$$

The concentrations of PC1 and PC2, as determined by the IAST model, were 83 percent and 13 percent of C_T, respectively. Therefore, out of the 14.7 mg/L of PC1, 7.8 mg/L is biodegradable, and 6.9 mg/L is non-biodegradable. Similarly, the concentration of PC2 is 2.3 mg/L, 1.2 mg/L of which is biodegradable, and 1.1 mg/L is non-biodegradable.

Based on the above analysis, the ozonated NOM solution consists of five components, two which are adsorbable and biodegradable, two which are adsorbable and non-biodegradable, and one which is biodegradable and non-adsorbable. A summary of the concentrations and adsorption parameters for the components of ozonated NOM is given in Table 7.3.

Table 7.3. Characterization of Ozonated NOM.

Component	$\%C_T(0)$	Initial Concentration (mg/L)	Adsorption Parameters (K,1/n)
PC 1-A/B	44	7.8	8.4,0.084
PC 1-A/NB	39	6.9	8.4,0.084
PC 2-A/B	7	1.2	36.5,0.253
PC 2-A/NB	6	1.1	36.5,0.253
PC-NA/B	4	0.7	NA

For simplicity, since PC-NA/B accounts for only four percent of the feed TOC concentration, it was combined with PC1-A/B.

The composition of the resulting model NOM solution is shown in Table 7.4.

Table 7.4 Composition of Model NOM Solution

Component	$\%C_T(0)$	Initial Concentration (mg/L)	Adsorption Parameters (K,1/n)
PC 1-A/B	48	8.5	8.4,0.084
PC 1-A/NB	39	6.9	8.4,0.084
PC 2-A/B	7	1.2	36.5,0.253
PC 2-A/NB	6	1.1	36.5,0.253

CHAPTER 8. MULTICOMPONENT MODELING OF NOM

8.1 Multicomponent Adsorption and Biodegradation (MCAB) Model

A mathematical model was used to model the performance of the continuous flow recycle reactor (with GAC media) used for the biostabilization of ozonated NOM (see Chapter 6), and to draw inferences concerning the behavior of the ozonated NOM in a biologically active GAC reactor. The multicomponent adsorption and biodegradation (MCAB) model used in this research was written by Joseph Pedit (1988), PhD student in the Department of Environmental Science and Engineering at the University of North Carolina at Chapel Hill.

The MCAB model is based on the single component model developed by Chang and Rittmann (1987) to study the adsorption and biodegradation of a single solute in a fixed bed completely mixed reactor. The MCAB model is capable of handling up to four solutes, each possessing different adsorption and biodegradation characteristics, using a finite element solution technique instead of the orthogonal collocation method used by Chang and Rittmann. The GAC

media is assumed to consist of homogeneous, spherical particles. The biofilm is also homogeneous, with a constant density throughout. The model accounts for diffusion through the liquid film, biofilm, and GAC.

Adsorption is considered completely reversible. Competitive adsorption is modelled according to ideal adsorbed solution theory, using Freundlich adsorption parameters for the components of concern.

Biodegradation is governed by Monod kinetics, and occurs only in the solution phase and the biofilm. No biological activity takes place in the carbon particle. The thickness of the biofilm can increase or decrease in response to biological growth or shearing of attached bacteria, respectively. Table 8.1 contains the input necessary to run the model, a brief description, and the units of the parameters. The computer program for the MCAB model is provided on a disk at the end of this report. Grimberg (1989), who also used the MCAB model, provides documentation as an appendix to his report.

TABLE 8.1. Description of Input to MCAB Model

PARAMETER	DESCRIPTION	UNITS
NUMERICAL METHOD PARAMETERS		
NSOL	# OF SOLUTES	
NEAC	ELEMENTS IN GAC	
NEBF	ELEMENTS IN BIOFILM	
NGAUS1	# OF GAUSS QUAD. POINTS	
NGAUS2	# OF GAUSS QUAD. POINTS	
H	SIZE OF FIRST TIME STEP	(hr)
TOL	ERROR TOLERANCE	
NTYPE	TYPE OF TIME STEP	
NSTEP	# OF TIME STEPS	
TIME	TIME OF SIMULATION	(hr)
REACTOR PARAMETERS		
Q	FLOWRATE	(cm^3/hr)
VOL	EMPTY BED VOLUME	(cm^3)
RAD	RADIUS OF GAC PARTICLE	(cm)
RHO	GAC DENSITY	(g/cm^3)
XW	GAC DRY WEIGHT	(g)
XF	BIOFILM DENSITY	(g/cm^3)
B	COEFF. OF DECAY	(hr^{-1})
B_S	SHEAR COEFFICIENT	(hr^{-1})
BETA	g CO_2-C/g CELL-C DESTROYED	(g/g)
SOLUTE PARAMETERS		
DS	SURFACE DIFFUSIVITY	(cm^2/hr)
K	FREUNDLICH K	
1/n	FREUNDLICH n	
DF	FILM DIFFUSIVITY	(cm^2/hr)
KF	LIQ. FILM MASS TRANS COEFF.	(cm/hr)
K_S	HALF VELOCITY CONSTANT	(mg/L)
K_m	MAX. VELOCITY	(g/g cell-hr)
Y	YIELD COEFF.	(g CELL-C/g TOC)
A	g CO_2/g TOC CONSUMED	(g/g)
S_O	FEED CONC.	(mg/L)
INITIAL CONDITIONS		
ACSTAR	INIT. SOLUTE CONC. IN GAC	(g/g)
SBSTAR	INIT BULK PHASE CONC.	(g/cm^3)
C_O	FEED CO2	(g/cm^3)
COSTAR	INIT BULK PHASE CO^2 CONC.	(g/cm^3)
XSSTAR	INIT LIQ. PHASE BIOMASS	(g/cm^3)
LFSTAR	INIT BIOFILM THICKNESS	(cm)

8.2 Sensitivity Analysis

8.2.a Selection of Standard Input Parameters

The sensitivity of the MCAB model to selection of the Monod biokinetic parameters, k_m and K_s, and the Freundlich parameter K, was determined. These parameters were considered the most likely to vary among the pseudo-components into which the NOM was divided for modeling purposes. The focus of analysis was on how characterization of the pseudo-components affects their effluent concentration profiles and not on the assumptions regarding biofilm or mass transfer characteristics.

To most easily distinguish the effects of varying the selected parameters, a simple standard model solution was chosen, consisting of two components. One component was adsorbable but non-biodegradable (Component A/NB), and the other biodegradable but non-adsorbable (Component NA/B). Both components will diffuse into the biofilm, but only Component NA/B will be biodegraded, and cause the biofilm to grow. Similarly, only Component A/NB will be able to enter the GAC. Therefore, the two components will not compete with each other for adsorption sites. In Section 8.2.F, however, the issue of competitive adsorption is addressed. The standard input parameters are shown in Table 8.2. A summary of the parameter values for the sensitivity analysis is presented in Table 8.3.

TABLE 8.2 Standard Input Parameters Used in MCAB Model

NUMERICAL METHOD PARAMETERS

NSOL	2	
NEAC	2	
NEBF	1	
NGAUS1	10	
NGAUS2	10	
H	1.00E-08	(hr)
TOL	1.00E-06	
NTYPE	0	
NSTEP	480	
TIME	240	(hr)

REACTOR PARAMETERS

Q	83.3	(cm^3/hr)
VOL	69.0	(cm^3)
RAD	2.49E-02	(cm)
RHO	7.0E-01	(g/cm^3)
XW	3.8	(g)
XF	3.42E-03	(g/cm^3)
B	2.83E-03	(hr^{-1})
B_S	4.38E-03	(hr^{-1})
BETA	1.0	(g CO_2-C/g CELL-C)

SOLUTE PARAMETERS

	COMPONENT A/NB	NA/B	
DS	7.2E-07	7.2E-07	(cm^2/hr)
K	0.01	10.0	
1/n	0.60	0.60	
DF	5.76E-03	5.76E-03	(cm^2/hr)
KF	26.0	26.0	(cm/hr)
K_s	3.0	3.0	(mg/L)
k_m	1.88	0.00	(g/g cell-hr)
Y	0.68	0.68	(g CELL-C/g TOC)
A	0.32	0.32	(g/g)
S_0	3.0E-06	4.0E-06	(mg/L)

INITIAL CONDITIONS

ACSTAR	0.00	0.00	(g/g)
SBSTAR	0.00	0.00	(mg/L)
C_O	0.00		(mg/L)
COSTAR	0.00		(mg/L)
XSSTAR	5.30E-03		(mg/L)
LFSTAR	2.50E-05		(cm)

TABLE 8.3 Summary of Model Runs.

RUN	PARAMETER VALUES
1A	K(A/NB) = 5 (Freundlich)
1B	K(A/NB) = 10
1C	K(A/NB) = 15
1D	K(A/NB) = 20
1E	K(A/NB) = 25
2A	k_m = 0.5 mg TOC/mg Cell-hr
2B	k_m = 1.0
2C	k_m = 1.5
2D	k_m = 3.0
3A	K_s = 1.0 mg/L (for biodegradable component)
3B	K_s = 3.0
3C	K_s = 5.0
3D	K_s = 7.0
4A	K(NA/B)* = 0.01 (FREUNDLICH)
4B	K(A/B)** = 1.0
4C	K(A/B)** = 10.0

* 0.01 chosen to represent negligible adsorbability
** formerly component NA,B

8.2.b MCAB Model Output for Standard Input Parameters

The model results for the standard input case of the sensitivity analysis are shown in Figure 8.1. All concentrations have been normalized, expressed as a fraction of the influent TOC. The plot of the base case contains curves for the breakthrough of each pseudo-component, their sum, and the TIC (CO_2) production (expressed as C) resulting from biological activity.

The most prominent feature of the C_T plot is the "hump" near the beginning of reactor operation. This was noted experimentally by DeWaters (1987), using the same NOM as feed to a biologically active GAC reactor (shown in Figure 6.5). The "hump" is thought to be the combined result of the initial increase and subsequent decrease in the concentration profile of Component NA/B and the increasing concentration profile of Component A/NB. Thus, its shape and height should be functions of the biodegradation and adsorption parameters of NOM. In one experiment by DeWaters (run 4: 1 mg O_3/mg TOC; TOC=7 mg/L; EBCT=3.8 min.), the hump occurred between 0 and 20 hours (DeWaters, 1987). In the standard input case of this analysis, the hump is sharper and lasts from 0 to 10 hours.

Following the "hump", C_T begins to rise due to breakthrough of Component A/NB. Biodegradation of Component A/B has reached steady-state, as evidenced by the plateau in the TIC curve.

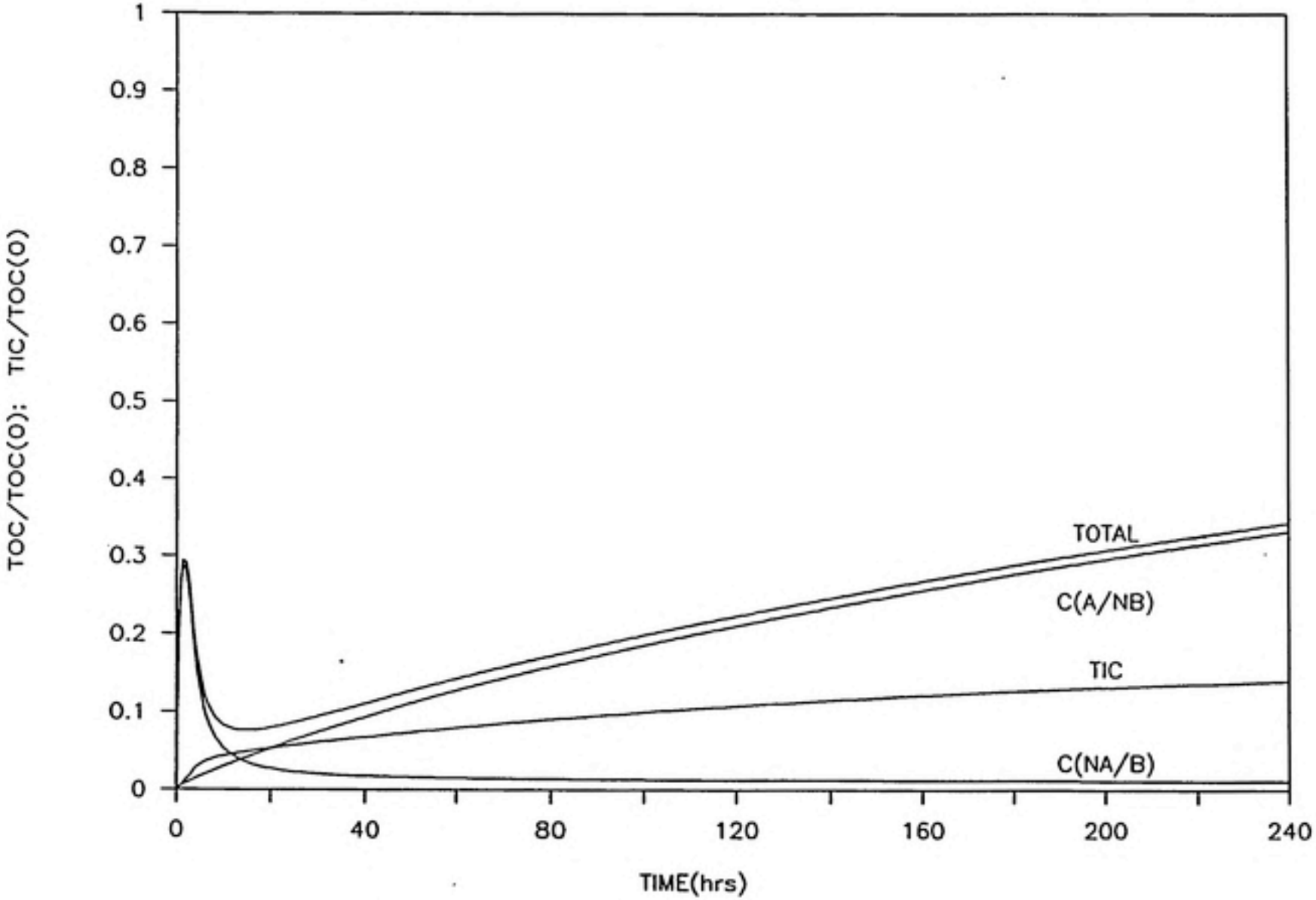

Figure 8.1 MCAB Model Results for Standard Input Parameters.

8.2.c Effect of Varying Freundlich K

The value of the Freundlich K parameter was varied between 2.5 and 40 (1/n constant throughout) to test the sensitivity of the model to changes in adsorbability. The breakthrough curves for C_T, presented in Figure 8.2.a, show that varying K primarily affects the shape of the breakthrough after the "hump". The breakthrough curves for each value of K are shown in Figure 8.2.b for Component NA/B and Component A/NB. For all values of K, the breakthrough curve for Component NA/B remains the same as in the case using standard input parameters. This is to be expected, because this component is biodegraded independently, and is unaffected by changes in the adsorbability of Component A/NB. The breakthrough curves for Component A/NB show that earlier breakthrough occurs as K is decreased, and determines the shape of the breakthrough curve after the "hump" when adsorption approaches exhaustion.

8.2.d Effect of Varying K_m

The C_T breakthrough curves produced by varying the maximum specific substrate utilization rate k_m (or u_m/Y) between 0.5 and 3.0 mg TOC/mg Cell-C/hr, are shown in Figure 8.3.a. Varying k_m has the most profound effect on the early stages of the breakthrough curve. The breakthrough curves

a)

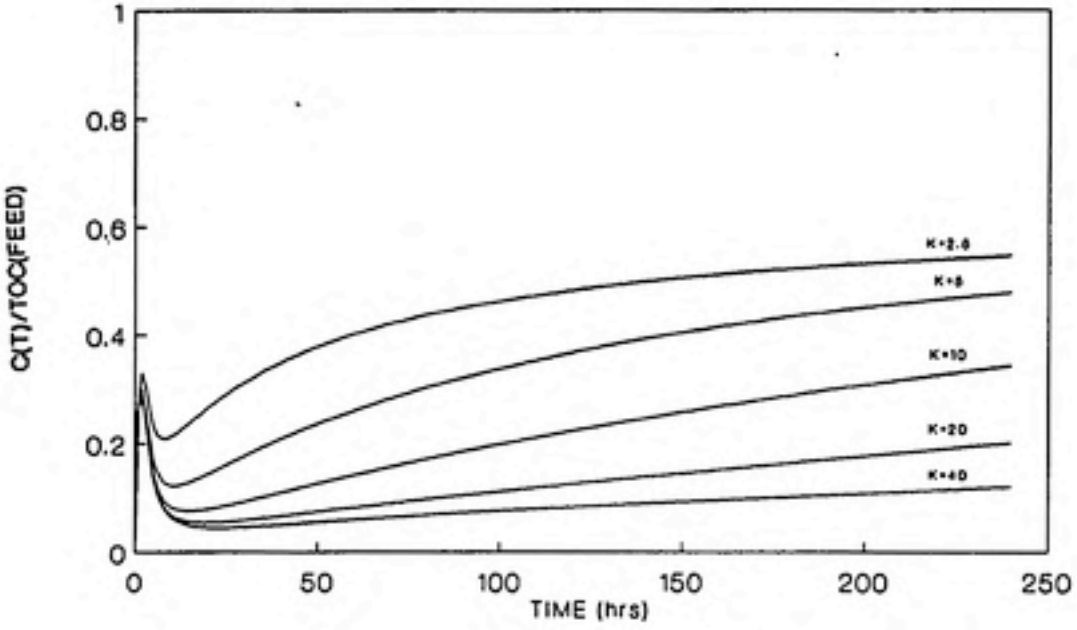

b)

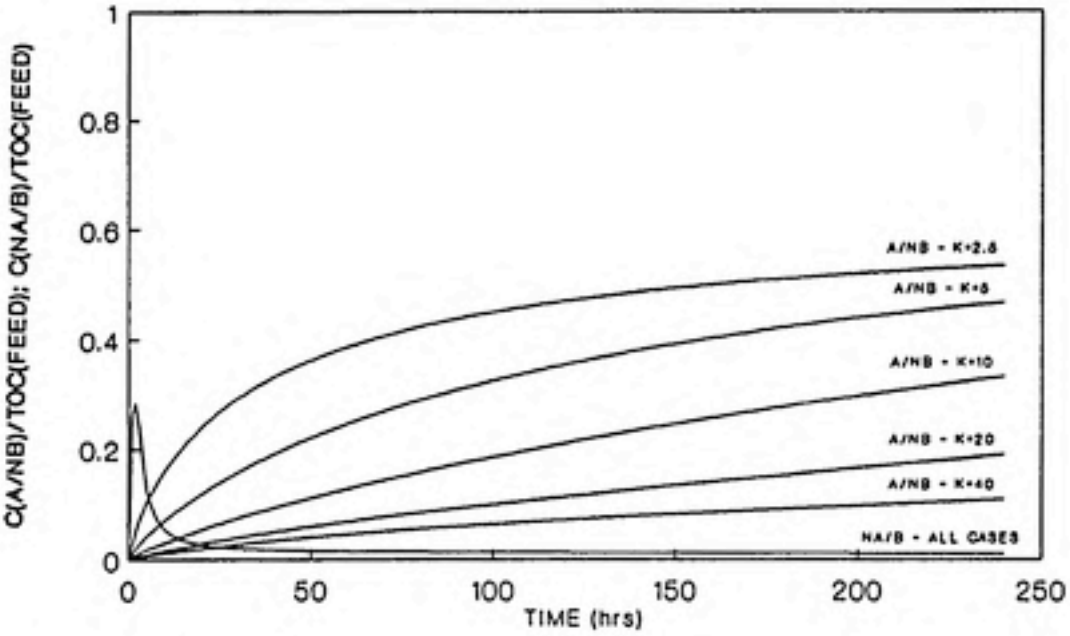

Figure 8.2 Effect on MCAB Model Results of Varying Freundlich K of Standard Input Parameters.

a)

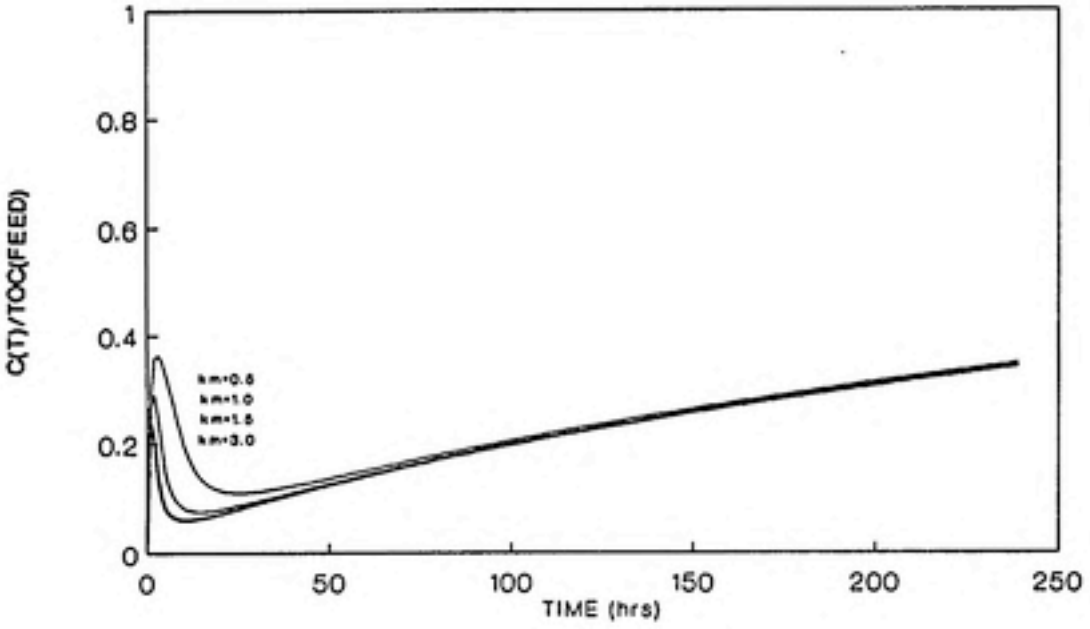

b)

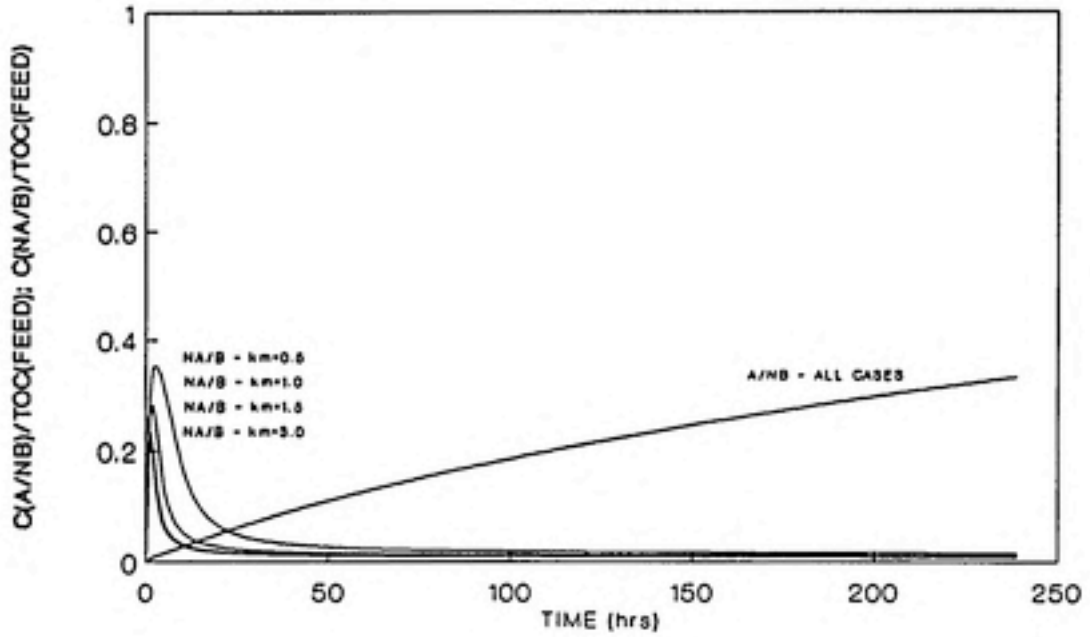

Figure 8.3 Effect on MCAB Model Results of Varying Maximum Specific Substrate Utilization Rate of Standard Input Parameters.

for Component NA/B and Component A/NB are shown in Figure 8.3.b. For lower values of K_m, more time is required for the biofilm to degrade Component NA/B to a steady-state effluent concentration. Therefore, the "hump" reaches a higher concentration and takes longer to tail off. A low value of K_m, when the yield coefficient is constant, must correspond to a low maximum specific growth rate, u_m. For this reason, it takes longer for the biomass initially present in the column to reach equilibrium. In addition, the lower reaction rate results in a slightly lower steady state removal of Component NA/B, hence a higher steady state effluent concentration. There is no change in the concentration profile of component A/NB as a result of varying the value of K_m for component NA/B.

8.2.e Effect of Varying K_S

The results of varying K_S between 1 and 7 mg TOC/L are contained in Figure 8.4 . The effect of varying K_S is similar to that of varying K_m, as increasing K_m and decreasing K_S both increase the biodegradation rate calculated from the Monod expression. As in the last case, a change in the value of K_S primarily affects the early stages of the breakthrough curve for C_T (Figure 8.4.a). For higher values of K_S, responsible for lower substrate utilization rates, the hump reaches higher concentrations and tails off more gradually. Also due to lower substrate

a)

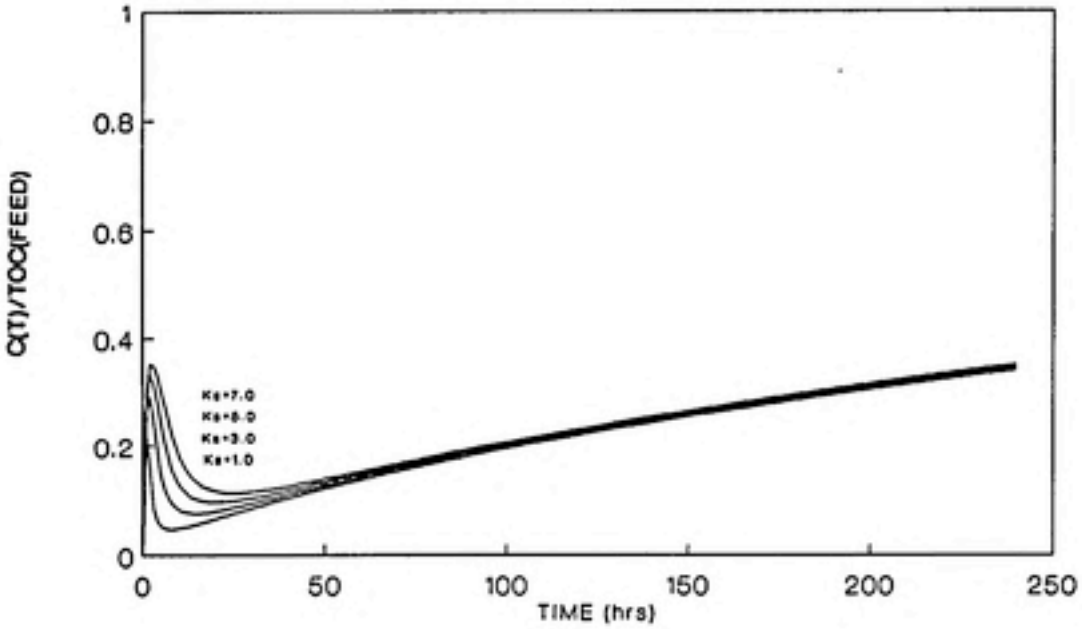

b)

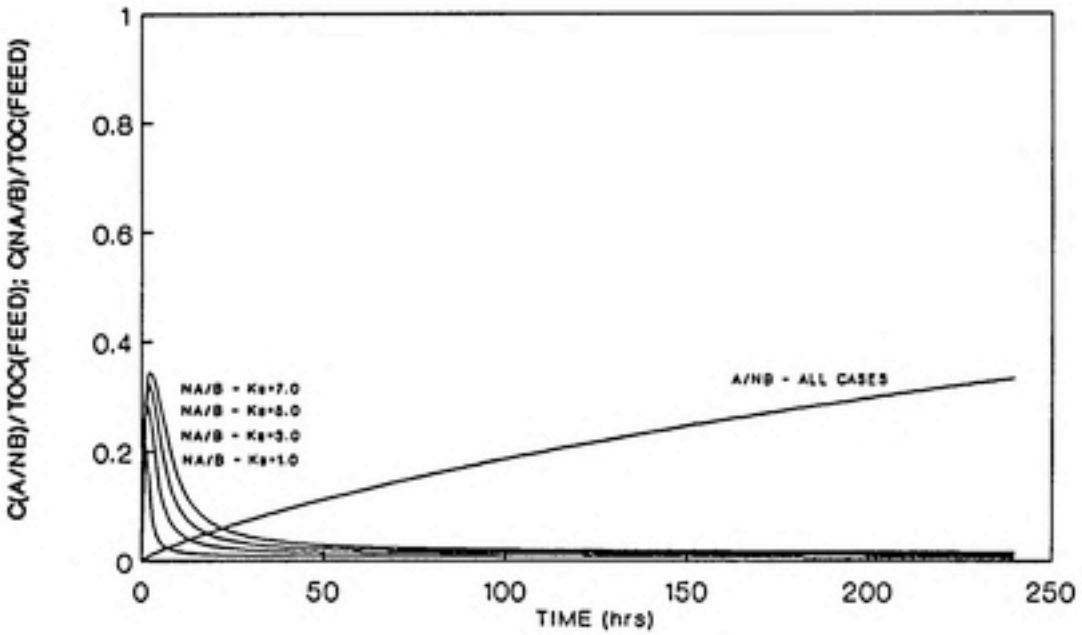

Figure 8.4 Effect on MCAB Model Results of Varying Monod Half Velocity Constant of Standard Input Parameters.

utilization rates, the microorganisms require a longer time to reduce Component NA/B to a steady-state concentration in the effluent (Figure 8.4.b). Slightly lower steady state removals, hence higher steady state effluent concentrations (Figures 8.4.b and 8.4.a), result from higher values of K_s. There is no change in the concentration profile of component A/NB as a result of varying the value of K_s for component NA/B.

8.2.f Effect of Varying Adsorbability of Component NA/B

For the cases presented in sections 8.2.b through 8.2.e the adsorbability of Component NA/B was negligible, less than the value of K for Component A/NB in all cases by a factor of 1000 to avoid competition for adsorption sites. Following these cases, the effect of making component NA/B adsorbable was tested, using the two component system consisting of Component A/NB and Component A/B (formerly Component NA/B).

The effect of varying K(A/B) between 0.01 and 10.0 (holding K(A/NB) constant at 10.0) on the breakthrough of C_T, Component A/B, and Component A/NB is shown in Figure 8.5.a. The breakthrough curves for a K(A/B) value of 0.01 represent the case using standard input parameters. The value of this parameter has a great impact on the shape of the "hump". The parameters found previously to affect the "hump", namely K_s and k_m, changed only the height of the

a)

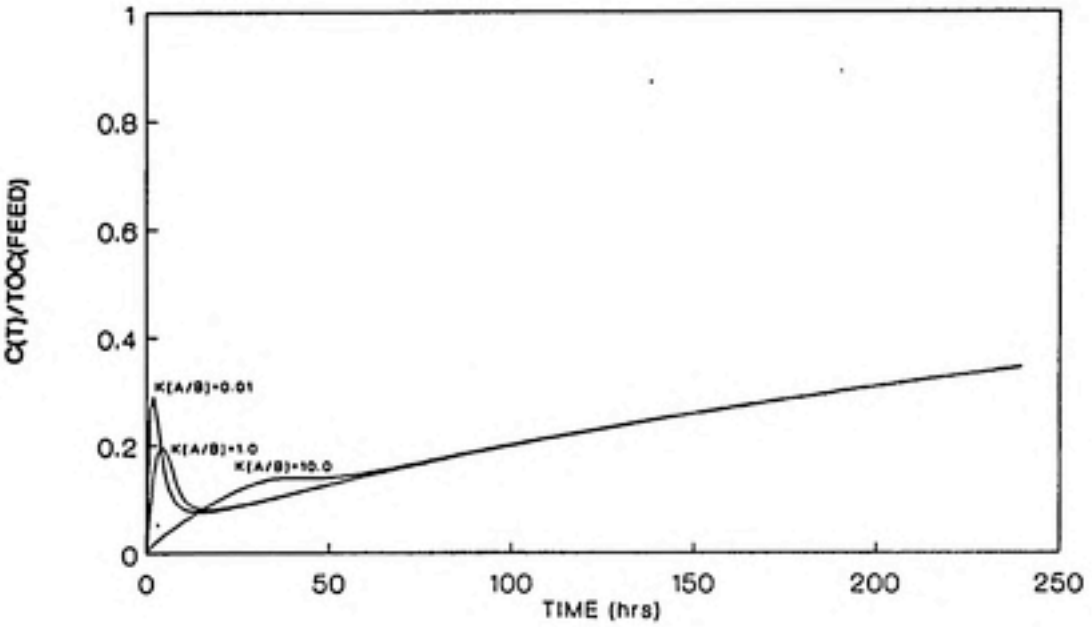

b)

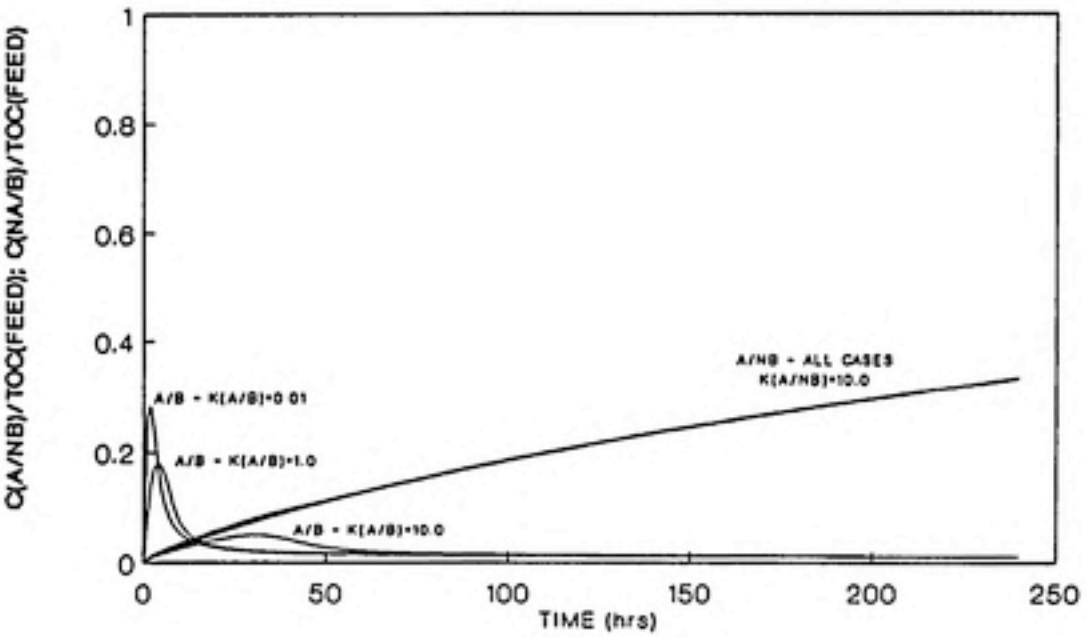

Figure 8.5 Effect on MCAB Model Results of Varying Freundlich K of Component NA/B in Standard Input Parameters.

peak and the time required for it to tail off, but had little effect on the starting point of the hump or its sharpness. Increasing the adsorbability of Component A/B (formerly Component NA/B), however, causes adsorption to account for a degree of removal of Component A/B until the biofilm becomes established, as shown in Figure 8.5.b. The concentration profile of component A/NB remains essentially unchanged, with the exception of a small degree of competitive adsorption evident between 0 and 50 hours.

The shape of the "hump" observed by DeWaters (1987), and presented in Figure 6.5, was not nearly as sharp as predicted when the biodegradable component was treated as non-adsorbable (i.e., Component NA,B). This supports the conclusions drawn from the isotherm results that a fraction exists in the ozonated NOM mixture which is both adsorbable and biodegradable.

8.3 Modeling of Experimental Results

The MCAB model was used to model the results of the continuous flow recycle containing GAC, which was used for the biostabilization of ozonated NOM (see Chap. 6). The run was modeled for the duration of the time when EBCT was held at 3.8 minutes (a total of about 300 hours). The model NOM solution consisted of four components, two being adsorbable and biodegradable (PC1-A/B and PC2-A/B) and the other two adsorbable and non-biodegradable (PC1-A/NB and PC2-A/NB).

The calculation of the concentration of each component is presented in Section 7.4.b. For these calculations, a value of 55 percent was used for the biodegradability of the ozonated NOM, as determined from the continuous flow GAC reactor used for the biostabilization.

The Monod biokinetic parameters used for PC1-A/B and PC2-A/B were from the batch biokinetic study. This study yielded a first-order rate constant, but the data were insufficient for determination of Monod parameters. For this reason, Monod parameters were calculated which forced the Monod equation to approximate first-order kinetics. These calculations are discussed in Section 5.3.c. A summary of the Freundlich adsorption parameters, Monod biokinetic parameters, and initial concentration of each component is presented in Table 8.4. The rest of the input to the model is shown in Table 8.5.

Table 8.4 Adsorption and biokinetic parameters of model NOM solution, assuming 55 percent biodegradability.

Component	Initial Concentration (mg/L)	Biokinetic Parameters (k_m,K_s)	Adsorption Parameters (K,1/n)
PC1-A/B	8.5	282,1752	8.4,0.084
PC1-A/NB	6.9	NA	8.4,0.084
PC2-A/B	1.2	282,1752	36.5,0.253
PC2-A/NB	1.1	NA	36.5,0.253

TABLE 8.5 Input Parameters for Test of MCAB Model with Experimental Data for Continuous Flow Recycle Reactor Assuming 55 Percent Biodegradability of NOM.

NUMERICAL METHOD PARAMETERS

NSOL	4	
NEAC	2	
NEBF	1	
NGAUS1	10	
NGAUS2	10	
H	1.00E-08	(hr)
TOL	1.00E-06	
NTYPE	0	
NSTEP	305	
TIME	305	(hr)

REACTOR PARAMETERS

Q	83.3	(cm^3/hr)
VOL	69.0	(cm^3)
RAD	2.49E-02	(cm)
RHO	7.0E-01	(g/cm^3)
XW	3.8	(g)
XF	3.42E-03	(g/cm^3)
B	3.60E-02	(hr^{-1})
BS	4.38E-03	(hr^{-1})
BETA	1.0	(g CO_2-C/g CELL-C)

SOLUTE PARAMETERS

	COMPONENT				
	1-A/B	1-A/NB	2-A/B	2-A/NB	
DS	7.2E-07	7.2E-07	7.2E-07	7.2E-07	(cm^2/hr)
K	8.4	8.4	36.5	36.5	
1/n	0.084	0.084	0.253	0.253	
DF	5.76E-03	5.76E-03	5.76E-03	5.76E-03	(cm^2/hr)
KF	26.0	26.0	26.0	26.0	(cm/hr)
K_s	1752	1752	1752	1752	(mg/L)
k_m	228	0.00	228	0.00	(g/g cell/hr)
Y	0.37	0.37	0.37	0.37	(g CELL-C/g TOC)
A	0.63	0.63	0.63	0.63	(g/g)
S_0	8.5	6.9	1.2	1.1	(mg/L)

INITIAL CONDITIONS

ACSTAR	0.00	0.00	0.00	0.00	(g/g)
SBSTAR	0.00	0.00	0.00	0.00	(g/cm^3)
CO	1.20				(mg/L)
COSTAR	0.00				(mg/L)
XSSTAR	5.30E-09				(g/cm^3)
LFSTAR	2.50E-05				(cm)

The model predictions for the case where 55 percent of NOM is assumed to be biodegradable are compared with the results of the continuous flow biostabilization experiment in Figure 8.6. The effluent TOC concentration and TIC production for the model results and the experimental data are shown in Figure 8.6.a as a fraction of the feed TOC concentration. In addition, the breakthrough of each component, their sum, and the TIC production are shown in Figure 8.6.b. The model predicts a more rapid initial breakthrough of TOC than the breakthrough shown by the experimental data. In addition, the hump in the predicted breakthrough curve takes longer to tail off than the hump exhibited by the data, although the hump in the experimental data is difficult to analyze due to the washout of GAC fines at the beginning of the run.

The model predicts a steady-state effluent TOC concentration of 49 percent of the feed TOC concentration. This is significantly less than the experimental steady-state value of 69 percent. In addition, the model overpredicted the TIC, or CO_2 production resulting from the biodegradation of the biodegradable components. One possible explanation for this was that the yield coefficient (Y) used was 0.37 mg Cell-C/mg TOC consumed, determined from the batch biokinetic study (Section 5.3.b). The apparent yield calculated using the experimental data from the continuous flow biostabilization experiment was 0.65 mg

a)

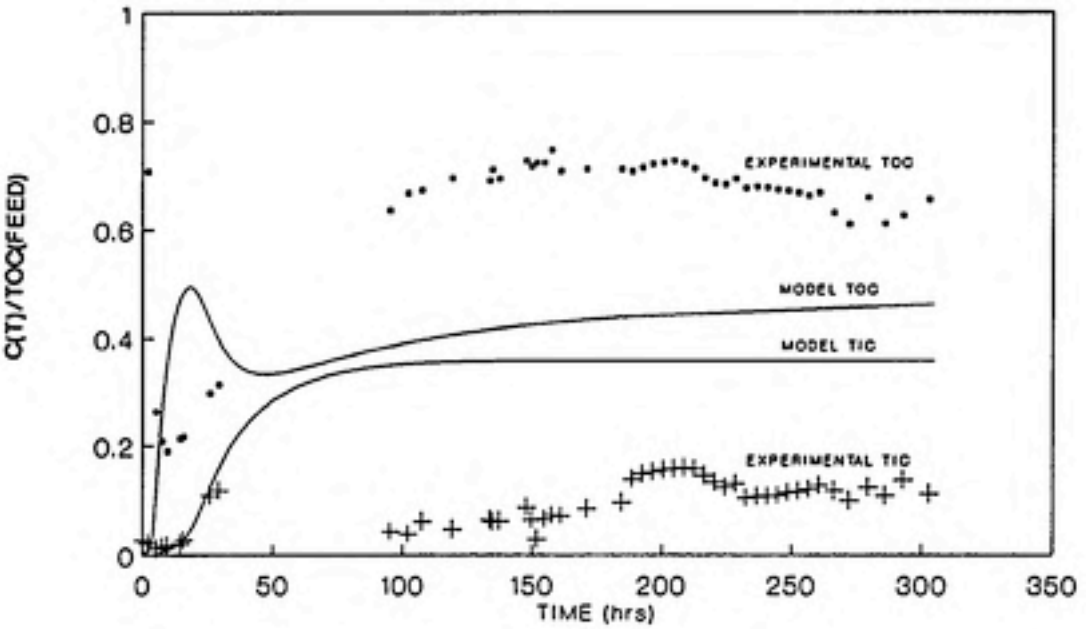

b)

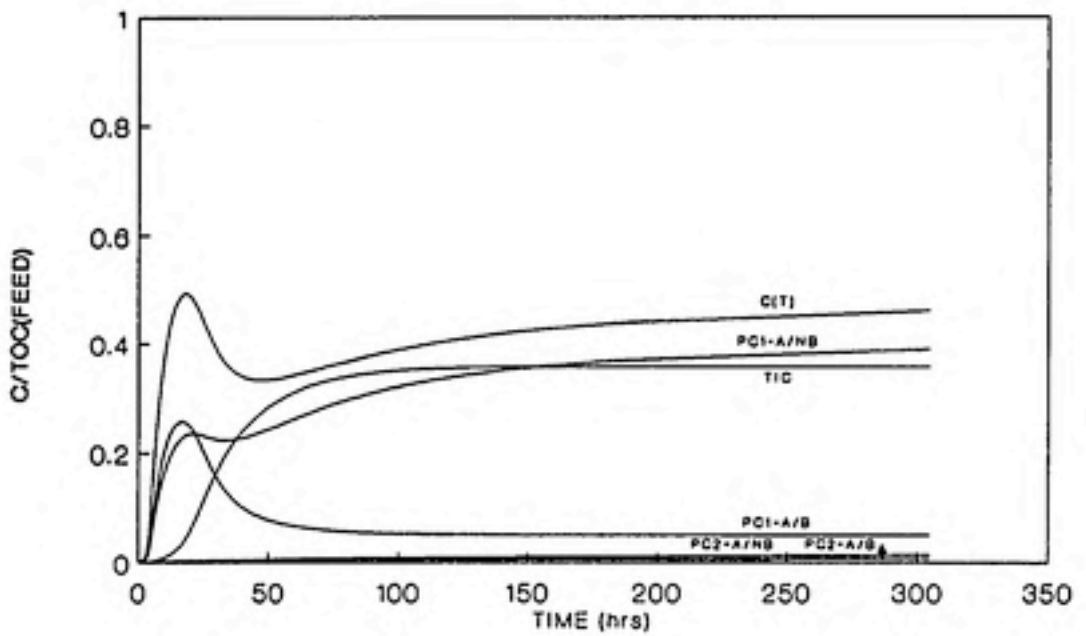

Figure 8.6 Comparison of MCAB Model Predictions for the 55 Percent Biodegradable NOM Solution and Results of the Continuous flow Biostabilization Experiment.

Cell-C/mg TOC consumed (Section 6.3). When substrate, CO_2, and biomass are all expressed in units of mg C/L, the unit CO_2 production resulting from biodegradation of TOC is given by Equation 8.1.

$$\text{Unit } CO_2 \text{ Production} = 1.0 - Y \qquad (8.1)$$

Using this equation, the CO_2 production per unit TOC reduction for the batch biokinetic experiment is 0.63, compared with a value of 0.35 for the biostabilization experiment. Therefore, the batch biokinetic results predict 80 percent more CO_2 production than the apparent yield calculated from the continuous flow biostabilization data for a given TOC removal.

Another possible explanation for the low steady-state effluent TOC concentration and high TIC production predicted by the model is that the biodegradability of the ozonated NOM was overpredicted in the GAC reactor. If biodegradation can not account for all of the steady-state TOC removal, then a portion of this removal must have been due to some other mechanism, such as slow adsorption.

To evaluate the effect of assuming that the long term TOC removal was solely due to biodegradation, another model run was performed assuming a lower percent removal of NOM by biodegradation. Only the concentrations and adsorption parameters from the ozonated NOM isotherm were used in these

calculations, as the ozonated-biostabilized NOM may have been affected by slow adsorption as well as biodegradation.

The concentrations of the ozonated-biostabilized NOM PCs, which were used in the determination of PC concentrations assuming 55 percent of NOM as biodegradable (Section 7.4.b), were not used in the calculations for the new assumption of percent biodegradability. The components of the ozonated NOM isotherm, first presented in Chapter 7, are shown again below for convenience:

IAST Equilibrium Model Results for Ozonated NOM

Component	K	1/n	%C(T)
Pseudo-component 1	8.44	0.084	83
Pseudo-component 2	36.54	0.253	13
Non-adsorbing Pseudo-component	--	--	4

The major difference between this modeling attempt and that presented in Figure 8.6 is the amount of NOM considered to be biodegradable. Here it is assumed that the ozonated NOM mixture was 15 percent biodegradable, as determined from the batch biokinetic study (Section 5.2). This value was not affected by adsorption, as no GAC was present. For this analysis it was also assumed that the difference in reactor configuration had no effect on the biodegradability of the ozonated NOM, contrary to the discussion in Section 6.2. It was furthermore assumed that this biodegradable fraction consisted of the least adsorbable material in the NOM mixture. Therefore, the non-adsorbable component was

entirely biodegradable, and was renamed PC NA/B. PC 1, the less adsorbable of the two adsorbing components, accounted for the remainder of the biodegradable fraction. Thus, PC 1 was split into a biodegradable (PC 1-A/B) and a non-biodegradable component (PC 1-A/NB). PC 2 was non-biodegradable, and became PC 2-A/NB. The components, plus their respective percentages of the initial TOC are shown in Table 8.6.

Table 8.6 Composition of Model NOM Solution Assuming 15 Percent Biodegradability

COMPONENT	$\%C_T(0)$
PC 1-A/B	11
PC 1-A/NB	72
PC 2-A/NB	13
PC-NA/B	4

For simplicity, since PC-NA/B accounts for only four percent of the total concentration, it was combined with PC 1-A/B. The concentrations, biokinetic parameters, and adsorption parameters of the revised model NOM solution are shown in Table 8.7. The rest of the input to the model is shown in Table 8.8.

Table 8.7 Adsorption and Biokinetic Parameters of Revised Model NOM Solution, Assuming 15 Percent Biodegradability of NOM.

Component	Initial Concentration (mg/L)	Biokinetic Parameters (k_m,K_s)	Adsorption Parameters (K,1/n)
PC 1-A/B	2.7	282,1752	8.4,0.084
PC 1-A/NB	12.7	NA	8.4,0.084
PC 2-A/NB	2.3	NA	36.5,0.253

The model predictions for the case where 15 percent of NOM is assumed biodegradable are compared with the results of the continuous flow biostabilization experiment in Figure 8.7. The total breakthrough and TIC production are plotted against the experimental results in Figure 8.7.a, and the effluent concentration profile of each component, TIC production, and total breakthrough are shown in Figure 8.7.b. Due to the lower concentration of biodegradable material, the hump is not as pronounced as in the previous case. The TOC again breaks through rapidly, and reaches steady-state at 81 percent of the feed TOC concentration, compared to 69 percent for the experimental results. The predicted TIC production is 10 percent of the feed TOC, approximately the same as the average experimental TIC production.

a)

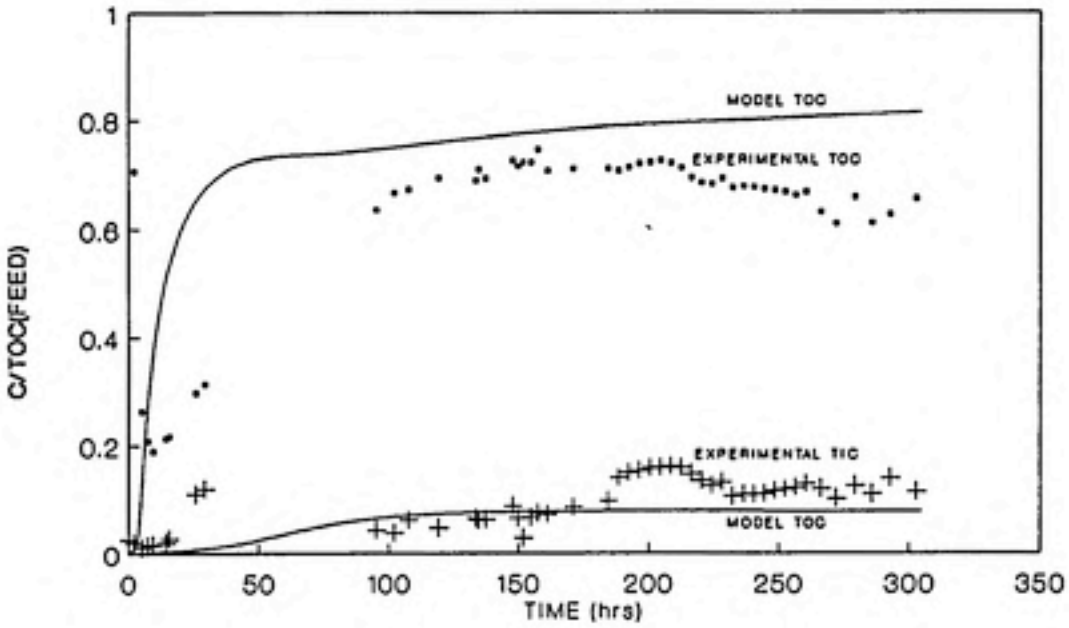

b)

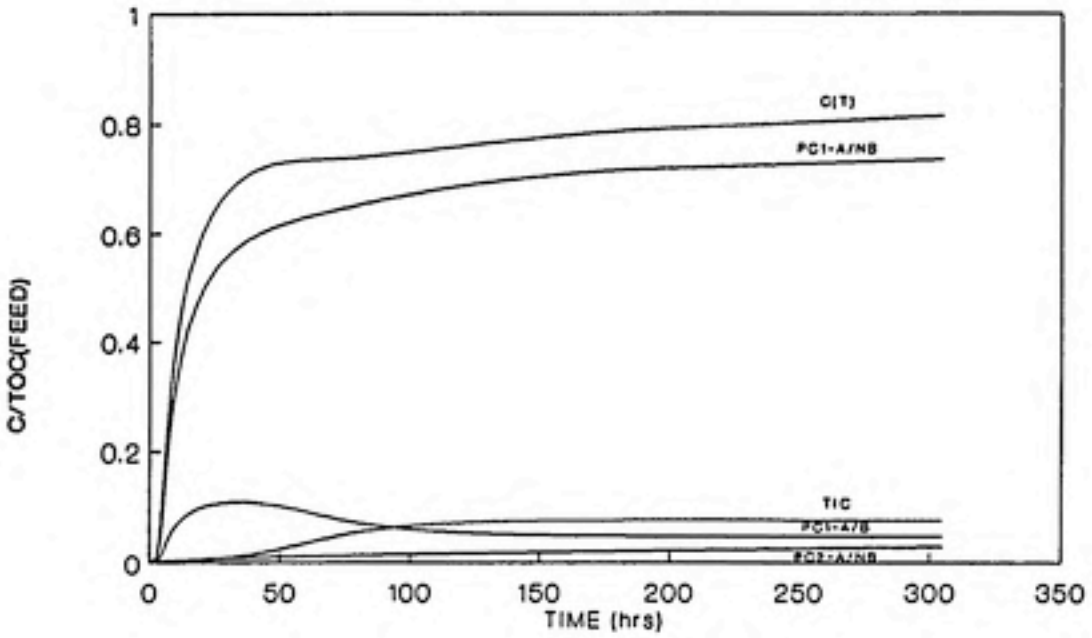

Figure 8.7 Comparison of MCAB Model Predictions for the 15 Percent Biodegradable NOM Solution and Results of the Continuous flow Biostabilization Experiment.

TABLE 8.8 Input Parameters for Test of MCAB Model with Experimental Data for Continuous Flow Recycle Reactor Assuming 15 Percent Biodegradability of NOM.

NUMERICAL METHOD PARAMETERS

NSOL	3
NEAC	2
NEBF	1
NGAUS1	10
NGAUS2	10
H	1.00E-08 (hr)
TOL	1.00E-06
NTYPE	0
NSTEP	305
TIME	305 (hr)

REACTOR PARAMETERS

Q	83.3	(cm^3/hr)
VOL	69.0	(cm^3)
RAD	2.49E-02	(cm)
RHO	7.0E-01	(g/cm^3)
XW	3.8	(g)
XF	3.42E-03	(g/cm^3)
B	3.60E-02	(hr^{-1})
BS	4.38E-03	(hr^{-1})
BETA	1.0	(g CO_2-C/g CELL-C)

SOLUTE PARAMETERS

	COMPONENT			
	1-A/B	1-A/NB	2-A/NB	
DS	7.2E-07	7.2E-07	7.2E-07	(cm^2/hr)
K	8.4	8.4	36.5	
1/n	0.084	0.084	0.253	
DF	5.76E-03	5.76E-03	5.76E-03	(cm^2/hr)
KF	26.0	26.0	26.0	(cm/hr)
K_s	1752	1752	1752	(mg/L)
k_m	228	0.00	0.00	(g/g cell/hr)
Y	0.37	0.37	0.37	(g CELL-C/g TOC)
A	0.63	0.63	0.63	(g/g)
S_0	2.7	12.7	2.3	(mg/L)

INITIAL CONDITIONS

ACSTAR	0.00	0.00	0.00	(g/g)
SBSTAR	0.00	0.00	0.00	(g/cm^3)
CO	1.20			(mg/L)
COSTAR	0.00			(mg/L)
XSSTAR	5.30E-09			(g/cm^3)
LFSTAR	2.50E-05			(cm)

CHAPTER 9. CONCLUSIONS AND RECOMMENDATIONS

9.1 Conclusions

1. An adsorption isotherm was determined from an equilibrium adsorption experiment using ozonated NOM. Ideal adsorbed solution theory (IAST) was used to obtain the Freundlich adsorption parameters for the pseudo-components of the NOM solution. The results suggest that the ozonated NOM may be described as a mixture of two adsorbing pseudo-components and one non-adsorbing pseudo-component.

2. Biostabilization of ozonated NOM proved difficult to identify. A batch recycle reactor achieved approximately 20 percent removal over 13 days. A 15 percent TOC removal was accomplished in the batch biokinetic study, over about six days. A continuous flow reactor with GAC media exhibited a TOC removal of 55 percent for a long empty bed contact time (51 minutes). As the adsorption capacity of the GAC had apparently reached exhaustion, this removal was attributed solely to biodegradation, and was used to define the biodegradable fraction of the ozonated NOM solution. Continuous flow reactors were used to compare biodegradation

on GAC and anthracite media. Due to unexplained TIC production with no corresponding decrease in TOC in the anthracite reactor, the GAC reactor was used to produce the desired biostabilized NOM.

3. An adsorption isotherm was determined for the ozonated-biostabilized NOM sample. The results indicate that the ozonated-biostabilized sample may be described by two adsorbing pseudo-components, and that no non-adsorbable pseudo-component was present. Isotherm results showed that biostabilization increased overall adsorbability of the mixture.

4. A batch biokinetic study was performed to determine Monod biokinetic parameters for use in the model. The data collected were insufficient to fit the Monod model, but first-order biokinetic parameters were obtained. Using these parameters, Monod parameters were calculated which forced the Monod equation to approximate first-order kinetics.

5. A multicomponent model was tested using the experimentally derived adsorption and biokinetic parameters. The concentrations of the NOM components were calculated using a value of 55 percent for the biodegradable fraction. For these conditions, the model underpredicted TOC breakthrough, possibly due to erroneous biokinetic

parameters. In addition, the model significantly overpredicted TIC production, due to the fact that the batch biokinetic results predict 80 percent more CO_2 production than the apparent yield calculated from the continuous flow biostabilization data for a given TOC removal.

6. The model was also tested using a value of 15 percent for the biodegradable fraction. This attempt slightly overpredicted TOC breakthrough, and predicted the TIC production well. These results suggest that biodegradation might not account for all of the 55 percent TOC removal accomplished by the continuous flow GAC reactor. Some other mechanism is suspected, such as slow adsorption.

9.2 Recommendations

1. Biostabilization should be accomplished using non-adsorbing media, thereby diminishing the possibility that mechanisms other than biodegradation are responsible for TOC removal.

2. Other methods, such as fractionation by gel permeation chromatography, should be evaluated for the characterization of NOM. It seems desirable to trace the same set of components through biostabilization, rather than define a new set of components, as is the case with IAST.

3. Biokinetic parameters should be determined using the same reactor configuration as that to be modeled. This would eliminate discrepancies in degradability and biokinetic parameters due solely to differences in reactors.

REFERENCES

Benedek, A., 1979. "Ozone and Activated Carbon Adsorption: A Mechanistic Analysis of Water Treatment Data," Ozonews, 6:1-6.

Bouwer, E.J., & Crowe, P.B., 1988. "Biological Processes in Drinking Water Treatment," Jour. AWWA, 80:9:82-93.

Brogden, W.B., 1971. "Characterization of Fresh Water and Estuarine Humic Acids by Molecular Weight Distribution," Ph.D. Dissertation, Florida State Univ., Tallahassee, Florida.

Chang, H.T., & Rittmann, B.E., 1987. "Mathematical Modeling of Biofilm on Activated Carbon," Environ. Sci. & Tech., 21:273-280.

Crittenden, J.C., Luft, P., & Hand, D.W., 1985. "Prediction of Multicomponent Adsorption Equilibria in Background Mixtures of Unknown Composition," Water Res., 19:12:1537-1548.

Davis, J.A., & Gloor, R., 1981. "Adsorption of Dissolved Organics in Lake Water by Aluminum Oxide: Effect of Molecular Weight," Envir. Sci. and Tech., 15:10:1223-1229.

DeWaters, J.E., 1987. "Biological Activity on Granular Activated Carbon in the Presence of Ozonated Naturally Occurring Humic Substances," Master's Report, Univ. of North Carolina, Chapel Hill, NC.

DiGiano, F.A., 1986. "Ozone and Biodegradation in Slow Sand Filters and Granular Activated Carbon," in AWWA preconference seminar: Ozonation: Recent Advances and Research Needs, pp. 1-24.

Frick, B.R., and Sontheimer, H., 1983. "Adsorption Equilibria in Multisolute Mixtures of Known and Unknown Composition," in Treatment of Water by Granular Activated Carbon, M.J. McGuire and I.H. Suffet, eds., Amer. Chem. Soc., Washington, D.C., pp. 247-268.

Gaudy, A.F., & Gaudy, E.T., 1980. "Microbiology for Environmental Scientists and Engineers, McGraw-Hill Book Company, New York, New York.

Glaze, W.H., & Wallace, J.L., 1984. "Control of Trihalomethane Precursors in Drinking Water: Granular Activated Carbon with and without Preozonation," Jour. AWWA, 76:2:68-75.

Glaze, W.H., Lin, C.C., Crittenden, J.C., & Cotton, R., 1986. "Adsorption and Microbiological Mechanisms for Removal of Natural Organics in Granular Activated Carbon Columns," Ozone Sci. and Eng., 8:299-319.

Grimberg, S.J., 1988. Personal Communication.

Grimberg, S.J., 1989. "Biofilm Growth and Biodegradation of Ozonated Natural Organic Matter on Granular Activated Carbon," Master's Report, Univ. of North Carolina, Chapel Hill, NC.

Harrington, G.W., DiGiano, F.A., 1989. "Adsorption Equilibria of Natural Organic Matter After Ozonation," Jour. AWWA, 81:6:93-101.

Harrington, G.W., DiGiano, F.A., and Fettig, J., 1989. "The Effect of Coagulation, Ozonation, and Biodegradation on the Activated Carbon Adsorption of Aquatic Humic Substances," in The Influence of Aquatic Humic Substances on the Fate and Treatment of Pollutants, I.H. Suffet and P. McCarthy, eds., Amer. Chem. Soc., Washington, D.C., pp. 727-746.

Hobbie, J.E., Daley, R.J., Jasper, S., 1977. "Use of Nuclepore Filters for Counting Bacteria by Fluorescence Microscopy," Applied and Env. Micro., 33:5:1225-1228.

Hubele, C., 1985. "Adsorption und Biologischer Abbau von Juminstaoffen in Aktivkohlefiltern," Publication No. 27, Department of Water Chemistry, Engler Bunte Institut, University of Karlsruhe, Karlsruhe, FRG.

Mallevialle, J., 1982 "The Degradation of Humic Substances in Water by Various Oxidizing Agents," Ozone Sci. and Eng., 4:1:33-44.

Maloney, S.W., Bancroft, K., Pipes, W.O., & Suffet, I.H., 1984. "Bacterial TOC Removal on Sand and GAC," Jour. ASCE Env. Eng. Div., 110:3:519-533.

James M. Montgomery Engineers, Inc., 1985. Water Treatment Principles and Design, John Wiley & Sons, Inc., pp. 67-70.

Myers, A.L., and Prausnitz, J.M., 1965. "Thermodynamics of Mixed Gas Adsorption," AIChE Jour., 11:1:121-127.

Namkung, E., & Rittmann, B.E., 1987a. "Removal of Taste- and Odor-Causing Compounds by Biofilms Grown on Humic Substances," Jour. AWWA, 79:7:107-112.

Namkung, E., & Rittmann, B.E., 1987b. "Evaluation of Bisubstrate Secondary Utilization Kinetics by Biofilms," Biotech. and Bioeng., 29:3:335-342.

Neukrug, H.M., Smith, M.G., Maloney, S.W., & Suffet, I.H., 1984. "Biological Activated Carbon - at What Cost?," Jour. AWWA, 76:4:158-167.

Pedit, J.A., 1988. Personal Communication, "Multicomponent Adsorption and Biodegration (MCAB) Model."

Peel, R.G., & Benedek, A., 1980. "Dual Rate Kinetic Model of Fixed Bed Adsorber," Jour. ASCE Env. Eng. Div., 106:EE4:797-813.

Radke, C.J., and Prausnitz, J.M., 1972. "Thermodynamics of Multi-Solute Adsorption from Dilute Liquid Solutions," AIChE Jour., 18:4:761-768.

Randtke, S.J., and V.L. Snoeyink, 1983, "Evaluating GAC Adsorptive Capacity," Jour. AWWA, 75:8:406-413.

Rook, J.J., 1974. "Formation of Haloforms during Chlorination of Natural Waters," J. Water Trtmnt. Exam., 23:2:234-243.

Scott, C.D., and Strandberg, G.W., 1986. "Microbial Solubilization of Coal," Biotech. Progress, 2:3:131-139.

Somiya, I., Yamada, H., Nozawa, E., & Mohri, M., 1983. "Studies on the Biodegradability and GAC Adsorbability of Micropollutants by Preozonation," Presented at the Sixth Ozone World Congress, Washington, D.C.

Speitel, G.E. Jr., DiGiano, F.A., 1987. "The Bioregeneration of GAC Used to Treat Micropollutants," Jour. AWWA, 79:1:64-73.

Speitel, G.E. Jr., Dovantzis, K., DiGiano, F.A., 1987. "Mathematical Modeling of Bioregeneration in GAC Columns," Jour. ASCE Env. Eng. Div., 113:1:32-48.

Speitel, G.E. Jr., Turakhia, M.H., & Lu, C.J., 1989. "Initiation of Micropollutant Biodegradation in Virgin GAC Columns," Jour. AWWA, 81:4:168-176.

Standard Methods for the Examination of Water and Wastewater, 17th edition, 1989. American Public Health Association - American Water Works Association - Water Pollution Control Federation.

Summers, R.S., Haist, B., Koehler, J., Ritz, J., Zimmer, G., & Sontheimer, H., 1989. "The Influence of Background Organic Matter on GAC Adsorption," Jour. AWWA, 81:5:66-74.

Symons, J.M., Bellar, T.A., Carswell, J.K., DeMarco, J., Kropp, K.L., Robeck, G.G., Seeger, D.R., Slocum, C.J., Smith, B.L., & Stevens, A.A., 1975. "National Organics Reconnaissance Survey for Halogenated Organics," Jour. AWWA, 67:11:634-647.

Veenstra, J.N., Barber, J.B., & Kahn, P.A., 1983. "Ozonation: Its Effect on the Apparent Molecular Weight of Naturally Occurring Organics and Trihalomethane Production," Ozone Sci. and Eng., 5:225-244.

Werner, P., & Hambsch, B., 1986. "Investigations on the Growth of Bacteria in Drinking Water," Water Supply, 4:227-232.

Ying, W., & Weber, W.J. Jr., 1978. "Bio-Physicochemical Adsorption Model Systems for Wastewater Treatment," Proceedings 33rd Purdue Industrial Waste Conference, pp. 128-141.

Zimmer, G., Brauch, H.J., & Sontheimer, H., 1989. "Activated Carbon Adsorption of Organic Pollutants," in The Influence of Aquatic Humic Substances on the Fate and Treatment of Pollutants, I.H. Suffet and P. McCarthy, eds., Amer. Chem. Soc., Washington, D.C., pp. 579-596.